Cell

Article

Activated Type 2 Innate Lymphoid Cells Regulate Beige Fat Biogenesis

Min-Woo Lee,[1,7] Justin I. Odegaard,[1,7] Lata Mukundan,[1] Yifu Qiu,[1] Ari B. Molofsky,[2] Jesse C. Nussbaum,[3] Karen Yun,[1] Richard M. Locksley,[3,4,5] and Ajay Chawla[1,6,*]

[1]Cardiovascular Research Institute, University of California San Francisco, San Francisco, CA 94158-9001, USA
[2]Department of Laboratory Medicine, University of California San Francisco, San Francisco, CA 94143-0795, USA
[3]Department of Medicine, University of California, San Francisco, CA 94143-0795, USA
[4]Department of Microbiology and Immunology, University of California, San Francisco, CA 94143-0795, USA
[5]Howard Hughes Medical Institute, University of California, San Francisco, CA 94143-0795, USA
[6]Departments of Physiology and Medicine, University of California San Francisco, San Francisco, CA 94158-9001, USA
[7]Co-first author
*Correspondence: ajay.chawla@ucsf.edu
http://dx.doi.org/10.1016/j.cell.2014.12.011

SUMMARY

Type 2 innate lymphoid cells (ILC2s), an innate source of the type 2 cytokines interleukin (IL)-5 and -13, participate in the maintenance of tissue homeostasis. Although type 2 immunity is critically important for mediating metabolic adaptations to environmental cold, the functions of ILC2s in beige or brown fat development are poorly defined. We report here that activation of ILC2s by IL-33 is sufficient to promote the growth of functional beige fat in thermoneutral mice. Mechanistically, ILC2 activation results in the proliferation of bipotential adipocyte precursors (APs) and their subsequent commitment to the beige fat lineage. Loss- and gain-of-function studies reveal that ILC2- and eosinophil-derived type 2 cytokines stimulate signaling via the IL-4Rα in PDGFRα$^+$ APs to promote beige fat biogenesis. Together, our results highlight a critical role for ILC2s and type 2 cytokines in the regulation of adipocyte precursor numbers and fate, and as a consequence, adipose tissue homeostasis.

INTRODUCTION

White adipose tissue (WAT) is a highly dynamic organ that responds to nutrient and environmental stress (Berry et al., 2014; Rosen and Spiegelman, 2006; Rosen and Spiegelman, 2014; Zeve et al., 2009). When mammals are in positive energy balance, WAT expands by hyperplasia and hypertrophy to store excess nutrients. In contrast, prolonged cold stress induces catabolic programs in WAT depots, in particular in the subcutaneous WAT (scWAT) of mice, to support thermogenesis (Harms and Seale, 2013; Wu et al., 2013). In this case, adrenergic stimulation of scWAT promotes tissue "browning" via induction of beige adipocytes that express the uncoupling protein 1 (UCP1). This de novo recruitment of beige adipocytes alleviates cold stress to restore thermal homeostasis (Nedergaard and Cannon, 2014). Despite progress in this field, the physiologic signals that regulate adipocyte precursor proliferation and their subsequent commitment to the beige adipocyte lineage remain poorly understood.

Fate mapping studies have led to the identification of progenitor or precursor cell populations that give rise to brown and beige adipocytes in adult mice. These studies have revealed that interscapular brown adipocytes arise from a mesodermal progenitor that transiently expresses the myogenic transcription factors Myf5 and Pax7 (Lepper and Fan, 2010; Seale et al., 2008). In contrast, beige adipocytes, which are found in WAT depots of mice, primarily arise from Myf5$^-$ PDGFRα$^+$ precursor cells (Sanchez-Gurmaches et al., 2012; Seale et al., 2008). Fate mapping studies by the Granneman laboratory have elegantly demonstrated that pharmacologic activation of the β3-adrenergic receptor stimulates the proliferation of PDGFRα$^+$ precursor cells, which subsequently differentiate into beige adipocytes (Lee et al., 2012). Interestingly, these PDGFRα$^+$ precursor cells can also give rise to white adipocytes in the setting of dietary obesity (Berry and Rodeheffer, 2013; Hudak et al., 2014; Lee et al., 2012; Wang et al., 2014), suggesting that environmental signals likely dictate the commitment of PDGFRα$^+$ precursor cells to the beige or white adipocyte lineage.

Exposure of adult animals to environmental cold stimulates the growth of thermogenic beige fat via activation of adrenergic signaling pathways (Harms and Seale, 2013; Wu et al., 2013). In contrast to interscapular BAT, we recently reported that the scWAT relies on a hematopoietic circuit consisting of eosinophils and alternatively activated macrophages for the maintenance of its adrenergic tone. In response to environmental cold, we found that eosinophil-derived interleukin (IL)-4 induces the expression tyrosine hydroxylase (TH), the rate-limiting enzyme in the synthesis of catecholamines, in alternatively activated macrophages (Nguyen et al., 2011; Qiu et al., 2014). Accordingly, genetic deletion of *Il4ra* or *Th* in myeloid cells significantly impaired the development of thermogenic beige fat in mice (Qiu et al., 2014). The observation that other browning factors, such as meteorin-like (METRNL) also utilize this pathway for their thermic effects (Rao et al., 2014), suggests that type 2 innate immunity might be integrally linked with the development of beige adipose tissue.

ILC2s, which are present in lymphoid and nonlymphoid tissues (Moro et al., 2010; Neill et al., 2010; Price et al., 2010),

orchestrate type 2 innate and adaptive immune responses in the setting of tissue damage, helminth infection, and allergen exposure (Koyasu and Moro, 2013; McKenzie et al., 2014; Walker et al., 2013). In these scenarios, the release of epithelial cell-derived cytokines IL-33, IL-25, and thymic stromal lymphopoietin (TSLP) results in the activation of ILC2s, which then secrete IL-5 and IL-13 to initiate type 2 immune responses (Cayrol and Girard, 2014; Licona-Limón et al., 2013). For instance, in the absence of ILC2s or IL-4/13, the allergen chitin is unable to promote recruitment of eosinophils or alternatively activated macrophages in the lungs (Van Dyken et al., 2014). In addition to their functions in immunity at mucosal sites, ILC2s have been identified in epididymal WAT (eWAT) of mice, where they sustain eosinophils and alternatively activated macrophages to promote glucose homeostasis (Molofsky et al., 2013). Since ILC2-derived IL-5 and IL-13 are critical for initiating type 2 immune responses, we asked whether these cells might also orchestrate the development of beige fat in mice.

Here, we report that administration of IL-33 results in accumulation and activation of ILC2s in the scWAT of mice to stimulate biogenesis of functional beige fat. Surprisingly, in an IL-4/13-dependent manner, IL-33 stimulates the proliferation of PDGFRα^+ adipocyte precursor cells, which then commit to the beige adipocyte lineage. The dependence of APs on IL-4/13 signaling for their expansion and commitment to beige adipocytes is not restricted to their pharmacological activation by IL-33 but is also observed during normal physiologic development of this tissue.

RESULTS

IL-33 Promotes Growth of Functional Beige Fat in Thermoneutral Mice

To investigate the functions of ILC2s in beige fat development, we intraperitoneally administered IL-33 to thermoneutral mice daily for 8 days to activate tissue resident ILC2s. In a dose-dependent manner, administration of IL-33 led to a robust increase in the expression of UCP1 protein in the scWAT of thermoneutral C57BL/6J mice (Figures 1A and 1B), suggesting that IL-33 stimulates the growth of beige fat. This browning of scWAT by IL-33 was comparable in magnitude to that induced by the type 2 cytokines IL-4 or IL-13 (Figure 1C), which previously have been implicated in the development of beige fat (Qiu et al., 2014; Rao et al., 2014). Histologic analysis confirmed the presence of multilocular beige adipocytes in the scWAT of mice treated with IL-33 (Figures 1D and 1E). In contrast to browning of scWAT, administration of IL-33, IL-13, or IL-4 did not alter the expression of UCP1 protein in the interscapular brown adipose tissue (BAT) of thermoneutral mice (Figure 1C). Together with our previous studies, these results demonstrate a selective role for type 2 cytokines in stimulating beige fat development.

Next, we asked whether IL-33-induced browning of scWAT contributes to whole-body energy expenditure. To test this postulate, we quantified energy expenditure in vehicle- and IL-33-treated mice at different environmental temperatures. Although energy expenditure was similar in vehicle- and IL-33-treated mice at thermoneutrality (30°C), animals treated with IL-33 had higher energy expenditure (~13%–17%) at the cooler housing temperatures (Figures 1F and 1G), which likely reflects activation of recruited beige fat. Moreover, these results are consistent with the previous reports demonstrating that beige fat thermogenesis is stimulated by cold exposure in both mice and humans (Qiu et al., 2014; van der Lans et al., 2013; Yoneshiro et al., 2013).

Based on these results, we next investigated whether IL-33 increases energy expenditure in a UCP1-dependent manner. For these experiments, thermoneutral C57BL/6J and congenic *Ucp1*$^{-/-}$ mice were administered IL-33 for 8 days (Figure 1A), and oxygen consumption was quantified after injection of norepinephrine (NE). Administration of NE, which activates all adrenoreceptors to maximally stimulate thermogenesis (Golozoubova et al., 2006), transiently increased oxygen consumption in thermoneutral C57BL/6J mice (Figure 1H). This NE-stimulated increase in metabolic rate was markedly enhanced in C57BL/6J mice that were administered IL-33 (Figure 1H). Importantly, IL-33-induced increase in oxygen consumption was completely absent in *Ucp1*$^{-/-}$ mice (Figure 1I), indicating that IL-33-induced recruitment of beige fat is critical for increasing the total thermogenic capacity of these mice.

IL-33 Stimulates Proliferation and Commitment of Adipocyte Precursors to the Beige Fat Lineage

To uncover the mechanisms by which IL-33 promotes browning of scWAT, we characterized the immune and precursor populations present in the scWAT of mice. For these studies, we used heterozygous Red5 (*Il5*$^{Red5/+}$, R5) mice, which express tandem dimer red fluorescent protein (tdTomato) from the translation initiation site of the endogenous *Il5* locus (Nussbaum et al., 2013), to monitor the fate and activation of ILC2s. ILC2s residing in the scWAT of mice were identified as being Lin$^-$ (CD11b$^-$CD4$^-$CD5$^-$Cd11c$^-$NK1.1$^-$)Thy1.2$^+$T1/ST2$^+$KLRG1$^+$ cells (Figure S1A available online). In mice administered IL-33, ILC2s but not eosinophils, basophils or mast cells were the dominant source of IL-5 (Figures S1B and S1C). Furthermore, daily treatment with IL-33 for 8 days increased the numbers (~22-fold) and activation (~5.4-fold) of ILC2s in the scWAT (Figures 2A and 2B). This increase in ILC2 activation was accompanied by tissue eosinophilia and proliferation of PDGFRα^+ APs (~14-fold, as assessed by intracellular staining for cell proliferation antigen Ki67) (Figures 2C–2E, S2A, and S2B). Since PDGFRα^+ APs are bipotential cells capable of differentiating into white or beige adipocytes (Lee et al., 2012), we hypothesized that IL-33 might stimulate beige fat biogenesis by enhancing the commitment of APs to the beige fat lineage. To test this idea, we used flow cytometry to monitor the expression of beige adipocyte markers (TMEM26 and CD137) on PDGFRα^+ APs (Wang et al., 2014; Wu et al., 2012). We found that treatment with IL-33 increased the expression of TMEM26 and CD137 on the cell surface of PDGFRα^+ APs (Figures 2F, 2G, S2C, and S2D), suggesting that IL-33 enhances the growth of beige fat by altering the proliferative and differentiation potential of scWAT APs.

We next investigated the signaling pathways by which IL-33 stimulates the expansion of APs. We hypothesized that IL-33 itself or factors secreted by IL-33 activated ILC2s, such as IL-5

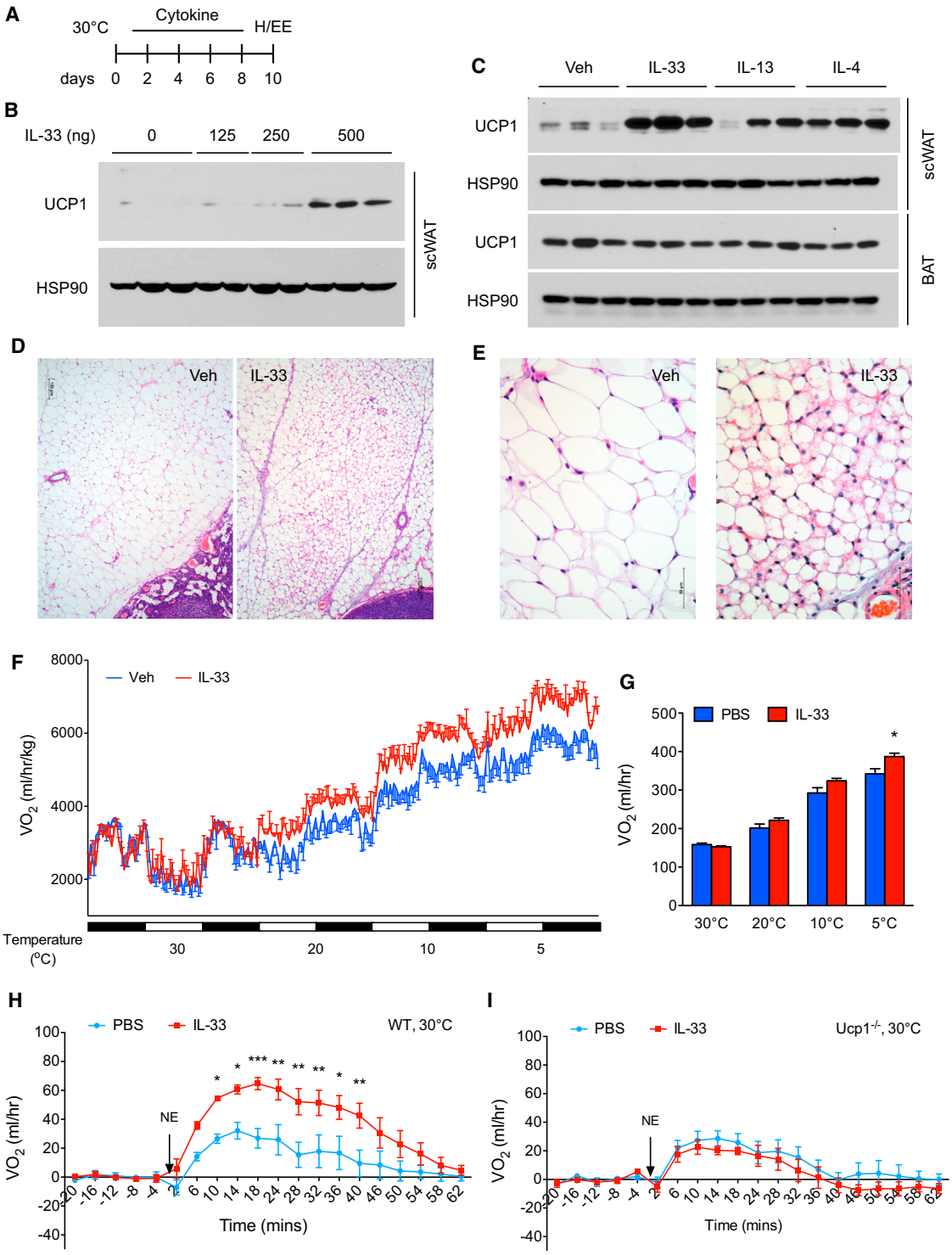

Figure 1. IL-33 Promotes Growth of Functional Beige Fat in Thermoneutral Mice

(A) Schematic for cytokine administration and metabolic analysis in thermoneutral mice.

(B) Immunoblotting for UCP1 in the scWAT of thermoneutral C57BL/6J administered various doses of IL-33 over 8 days (n = 2–3 per treatment dose).

(C) Immunoblotting for UCP1 in the scWAT and BAT of thermoneutral mice administered IL-33, IL-13, or IL-4 for 8 days (n = 3 per cytokine treatment).

(D and E) Representative sections of scWAT from thermoneutral C57BL/6J mice administered Vehicle (Veh) or IL-33 were stained with hematoxylin and eosin. (D) 100× magnification, (E) 400× magnification.

(legend continued on next page)

or IL-13 (Koyasu and Moro, 2013; McKenzie et al., 2014; Walker et al., 2013), directly stimulate the proliferation of PDGFRα$^+$ APs. Flow cytometric analysis revealed that PDGFRα$^+$ APs did not express the receptors required for signaling by IL-33 (IL1RL1) or IL-5 (IL-5Rα), but they did express IL-4Rα (Figures 2H–2J and S2E), which is required for both IL-13 and IL-4 signaling (Kelly-Welch et al., 2003). These observations led us to hypothesize that secretion of IL-13 by activated ILC2s or IL-4 by recruited eosinophils might support the proliferative burst of APs. We first tested the requirement for IL-5 in IL-33 stimulated AP proliferation. Albeit to a slightly lower extent than in WT mice, stimulation with IL-33 enhanced AP proliferation in R5R5 (*Il5*$^{Red5/Red5}$) homozygous mice (Figure S2F), which lack the eosinophil growth factor IL-5 but can secrete IL-13 upon activation (Figures S1D and S2G). Since eosinophils are an important source of IL-4 in WAT (Qiu et al., 2014; Wu et al., 2011), we next tested their requirement in IL-33-mediated AP proliferation. Figure S2H shows that IL-33 was equally efficacious in stimulating expansion of scWAT APs in eosinophil-deficient ΔdblGATA mice (Yu et al., 2002), suggesting potential redundancy between eosinophil-derived IL-4 and ILC2-dervied IL-13 in mediating this response. To test this hypothesis, we asked whether IL-33 could stimulate proliferation of APs in *Il4/13*$^{-/-}$ and *Il4ra*$^{-/-}$ mice. Indeed, administration of IL-33 failed to increase proliferation of APs in the scWAT of *Il4/13*$^{-/-}$ and *Il4ra*$^{-/-}$ mice (Figures 2K and 2L). A similar requirement for type 2 cytokine signaling was observed in IL-33-mediated browning of scWAT, as monitored by the expression of UCP1 protein in the scWAT of thermoneutral WT and *Il4ra*$^{-/-}$ mice administered IL-33 (Figure 2M). Together, these findings establish a hierarchy between ILC2s, eosinophils, and signaling via the IL-4Rα in the regulation of AP biology.

To test whether the stimulatory effects of IL-33 on AP proliferation and commitment require ILC2s, we administered IL-33 to *Rag2*$^{-/-}$ and *Rag2Il2rg*$^{-/-}$ mice, the latter known to lack ILC2s (Price et al., 2010). While IL-33 increased AP proliferation in *Rag2*$^{-/-}$ mice, it failed to do so in *Rag2Il2rg*$^{-/-}$ mice (Figure 2N), indicating an absolute requirement for ILC2s in IL-33-mediated expansion of scWAT APs. Similarly, the induction of beige adipocyte markers, TMEM26 and CD137, by IL-33 was only observed in *Rag2*$^{-/-}$ mice (Figures 2O, 2P, S2I, and S2J), suggesting that ILC2s are the likely target for IL-33-induced browning of scWAT.

Physiologic Expansion of Adipocyte Precursors Is Controlled by Type 2 Cytokine Signaling

Since pharmacologic activation of ILC2s promoted proliferation of adipogenic precursors in an IL-4/13-dependent manner, we next asked whether these signals might control the physiologic expansion of APs during the postnatal period. We first quantified the proliferative status of PDGFRα$^+$SCA1$^+$CD45$^-$CD31$^-$ APs in the scWAT of C57BL/6J mice at various ages (Figures S3A and S3B). We found that proliferation of scWAT APs, as assessed by intracellular staining for the cell proliferation antigen Ki67, was age dependent (Figure 3A). Approximately 5.8% of scWAT APs stained positive for Ki67 in 4-week-old mice, which declined by 85% and 95%, respectively, in the scWAT of 8- and 12-week-old mice (Figure 3A). BrdU incorporation experiments provided independent verification for this age-associated decline in DNA synthesis and AP proliferation (Figure 3B).

We next asked whether type 2 immunity regulates this postnatal expansion of APs in the WAT. In support of our hypothesis, we observed an age-associated decline in type 2 cytokine signaling in APs, as assessed by the phosphorylation status of signal transducer and activator of transcription 6 (STAT6), which mediates the biological effects of type 2 cytokines IL-4 and IL-13 (Figure 3C) (Kelly-Welch et al., 2003). Using 4get mice, which express green fluorescent protein (GFP) from the *Il4* locus (Mohrs et al., 2001), we next asked whether the number of cells competent for IL-4 production in scWAT changes with age. Congruent with the decrease in levels of pSTAT6 (Figure 3C), the scWAT of 9-week-old mice had ~70% fewer GFP$^+$ cells. This decrease in GFP$^+$ cells primarily reflected a decline in the numbers of resident eosinophils (Figure S3C), which have previously been implicated in secretion of IL-4 in scWAT and eWAT (Qiu et al., 2014; Wu et al., 2011). Furthermore, this reduction in numbers of GFP$^+$ eosinophils was associated with a ~70% decrease in proliferation (Ki67 positivity) and a ~50% reduction in numbers of APs present in the scWAT (Figures S3D and S3E). A similar age-associated decline in proliferation of APs was observed in the scWAT and eWAT of BALB/cJ mice (Figures S3F and S3G), suggesting that this is not a strain-specific effect. Finally, this age-associated decrease in AP proliferation was not a consequence of changes in expression of PDGFRα or IL-4Rα on the cell surface of APs (Figures S3H and S3I).

Based on these results, we next asked whether loss of type 2 cells or signals affects AP proliferation and numbers in the scWAT. For these studies, we focused on 5-week-old mice because we observed robust proliferation of APs at this age in both C57BL/6J and BALB/cJ mice. Consistent with our hypothesis, ΔdblGATA mice, which lack eosinophils, had ~30% fewer APs in their scWAT with ~70% lower proliferative fraction (Figures 3E and 3F). *Il4/13*$^{-/-}$ mice, which lack the type 2 cytokines IL-4 and IL-13, also demonstrated decreases in scWAT AP proliferation (~56%) and numbers (~70%) (Figures 3G and 3H). Similarly, deletion of the IL-4/13 signaling subunit *Il4ra* decreased the percentage of Ki67$^+$ APs by ~48% and their numbers by ~52% in scWAT (Figures 3I and 3J). In aggregate, these data suggest that signaling via the IL-4Rα accounts for ~50% of the proliferative capacity of APs in the scWAT of mice, prompting us to investigate the mechanisms by which type 2 immunity instructs the postnatal development and functions of this adipose depot.

(F) Cold-induced changes in oxygen consumption in thermoneutral C57BL/6J mice administered Vehicle (Veh) or IL-33 over 8 days (n = 4–5 per treatment).
(G) Oxygen consumption rate at various temperatures of C57BL/6J mice treated with Veh or IL-33 (n = 4–5 per treatment).
(H and I) Norepinephrine stimulated changes in oxygen consumption (VO_2) in conscious, thermoneutral C57BL/6J (H) and *Ucp1*$^{-/-}$ mice that were pretreated with vehicle (Veh) or IL-33 for 8 days (n = 5 per genotype and treatment). Data are represented as mean ± SEM.

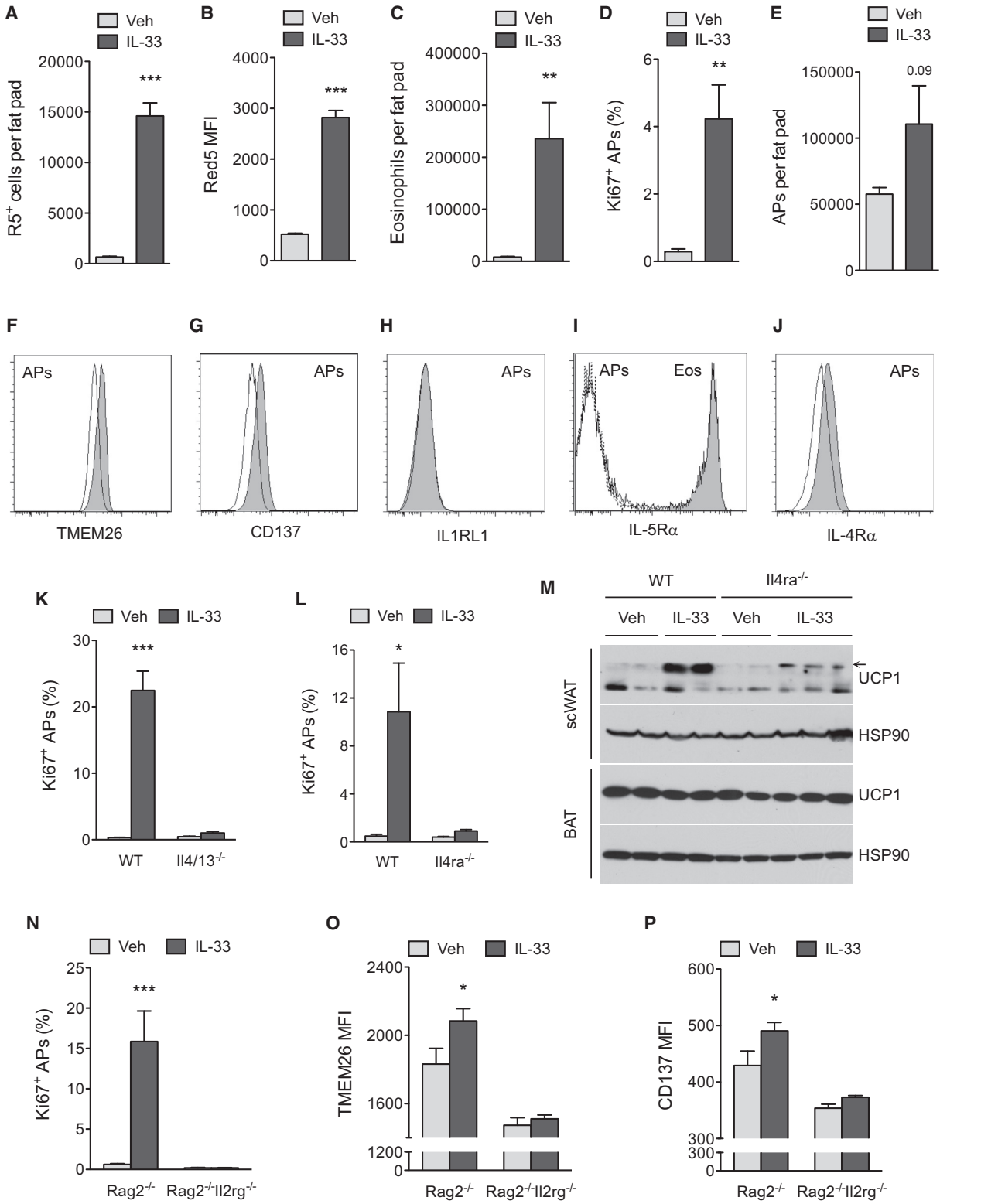

Figure 2. IL-33 Stimulates Proliferation and Commitment of Adipocyte Precursors to the Beige Fat Lineage

(A and B) Quantification of ILC2 numbers (A) and activation status (B) in the scWAT of thermoneutral, heterozygous Red5 (*Il5*$^{Red5/+}$) mice that were administered vehicle (Veh) or IL-33 for 8 days. Expression of IL-5 (td Tomato) from the Red5 allele was used as a marker of ILC2 activation (n = 9–10 per treatment).

(legend continued on next page)

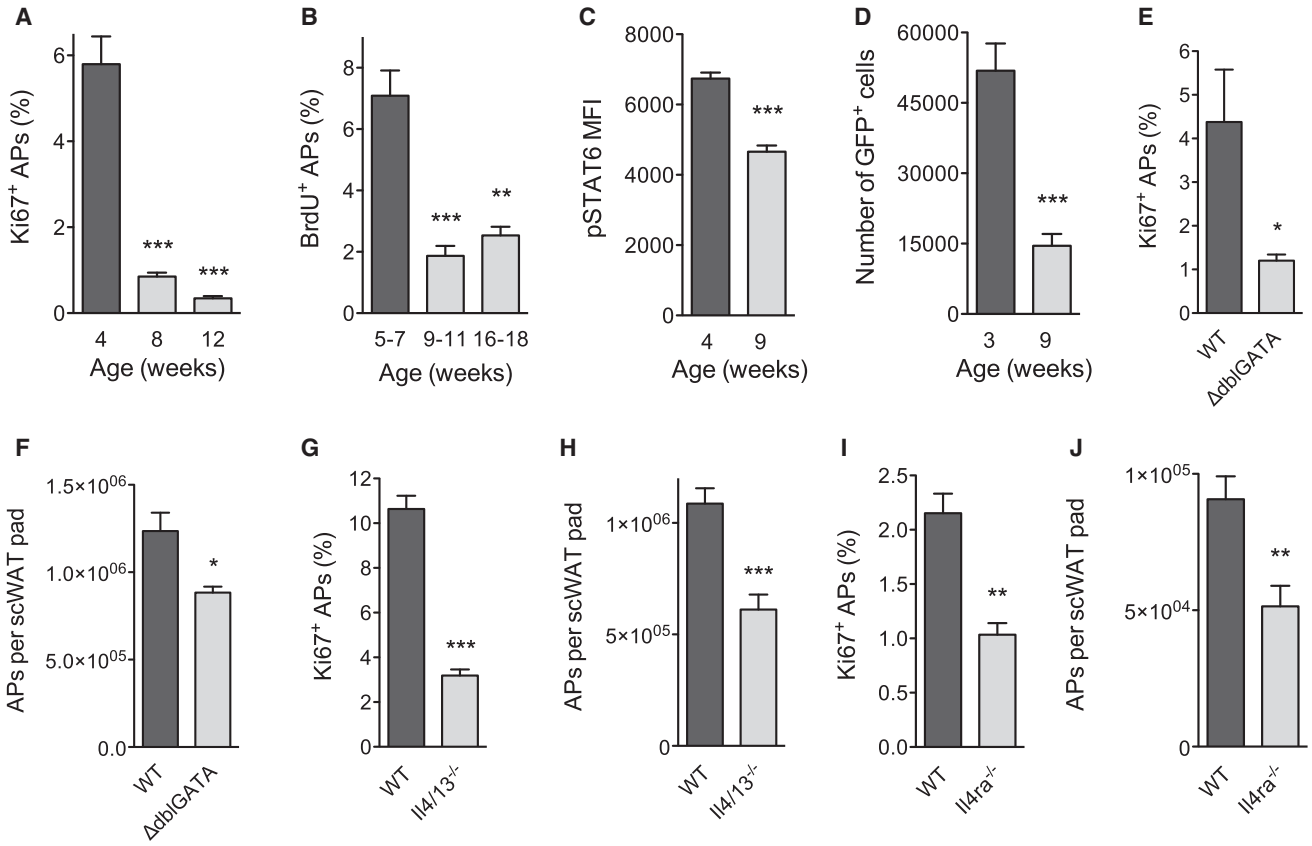

Figure 3. Type 2 Cytokine Signaling Controls Physiologic Expansion of Adipocyte Precursors

(A) Age-dependent proliferation of adipocyte precursors (APs) in the scWAT of C57BL/6J mice as assessed by intracellular staining for Ki67 (n = 4–5 per age).

(B) Age-dependent incorporation of BrdU by scWAT APs in C57BL/6J mice (n = 4–5 per age).

(C) Quantification of pSTAT6 levels in scWAT APs of C57BL/6J mice at different ages (n = 10–11 per age).

(D) Quantification of IL-4-producing cells in the scWAT of 4get mice at different ages. GFP expression marks cells competent for production of IL-4 (n = 5 per age).

(E–J) Quantification of Ki67$^+$ (E, G, and I) and total APs (F, H, and J) in scWAT of 5-week-old ΔdblGATA (E, F), *Il4/13*$^{-/-}$ (G and H), and *Il4ra*$^{-/-}$ (I and J) mice (n = 5–10 per genotype). Data are represented as mean ± SEM. See also Figure S3.

IL-4Rα Signaling in PDGFRα$^+$ Cells Promotes Expansion of Adipocyte Precursors

Previous studies by the Granneman laboratory have demonstrated that pharmacologic activation of the β3-adrenergic receptor stimulates the proliferation and differentiation of APs into beige adipocytes (Lee et al., 2012). Since we recently demonstrated that type 2 activation of macrophages via IL-4Rα stimulates release of norepinephrine in the scWAT and eWAT of mice (Nguyen et al., 2011; Qiu et al., 2014), we next asked whether myeloid cell IL-4Rα signaling might regulate the postnatal expansion and commitment of APs to the beige adipocyte lineage. To our surprise, we found that deletion of *Il4ra* in

(C) Quantification of eosinophils in the scWAT of thermoneutral heterozygous Red5 (*Il5*$^{Red5/+}$) mice that were administered Veh or IL-33 for 8 days (n = 8–10 per treatment).

(D) Quantification of adipocyte precursor (AP) proliferation in the scWAT of thermoneutral *Il5*$^{Red5/+}$ mice administered Veh or IL-33 for 8 days, as assessed by intracellular staining for Ki67 (D) and AP cell number per fat pad (n = 8–10 per treatment).

(F and G) Expression of beige adipocyte markers TMEM26 and CD137 on the scWAT APs of thermoneutral *Il5*$^{Red5/+}$ mice administered Veh or IL-33 for 8 days (n = 8–10 per treatment). Representative histograms for TMEM26 (F) and CD137 (G) are shown; clear histogram-Veh, shaded histogram-IL-33.

(H–J) Expression of IL1RLI (H), IL-5Rα (I), and IL-4Rα (J) on scWAT APs of mice. For IL1RL1 (H), the clear histogram represents WT APs, while the shaded represents *Il1rl1*$^{-/-}$ APs. For IL-5Rα (I), the dashed line histogram represents isotype, the solid line represents APs stained for IL-5Rα, and the shaded histogram represents eosinophils stained for IL-5Rα. For IL-4Rα (J), the solid line histogram represents isotype and the shaded histogram represents APs stained for IL-4Rα.

(K and L) Quantification of IL-33 induced AP proliferation in the scWAT of *Il4/13*$^{-/-}$ (K) and *Il4ra*$^{-/-}$ (L) mice (n = 4–8 per genotype and treatment).

(M) Immunoblotting for UCP1 in the scWAT and BAT of thermoneutral WT and *Il4ra*$^{-/-}$ mice administered IL-33 for 8 days (n = 2–3 per genotype and treatment).

(N–P) Quantification of AP proliferation (N), TMEM26 (O) and CD137 (P) expression in *Rag2*$^{-/-}$ and *Rag2*$^{-/-}$*Il2rgc*$^{-/-}$ mice treated with IL-33 (n = 6–8 per genotype and treatment).

Data are represented as mean ± SEM. See also Figure S1 and S2.

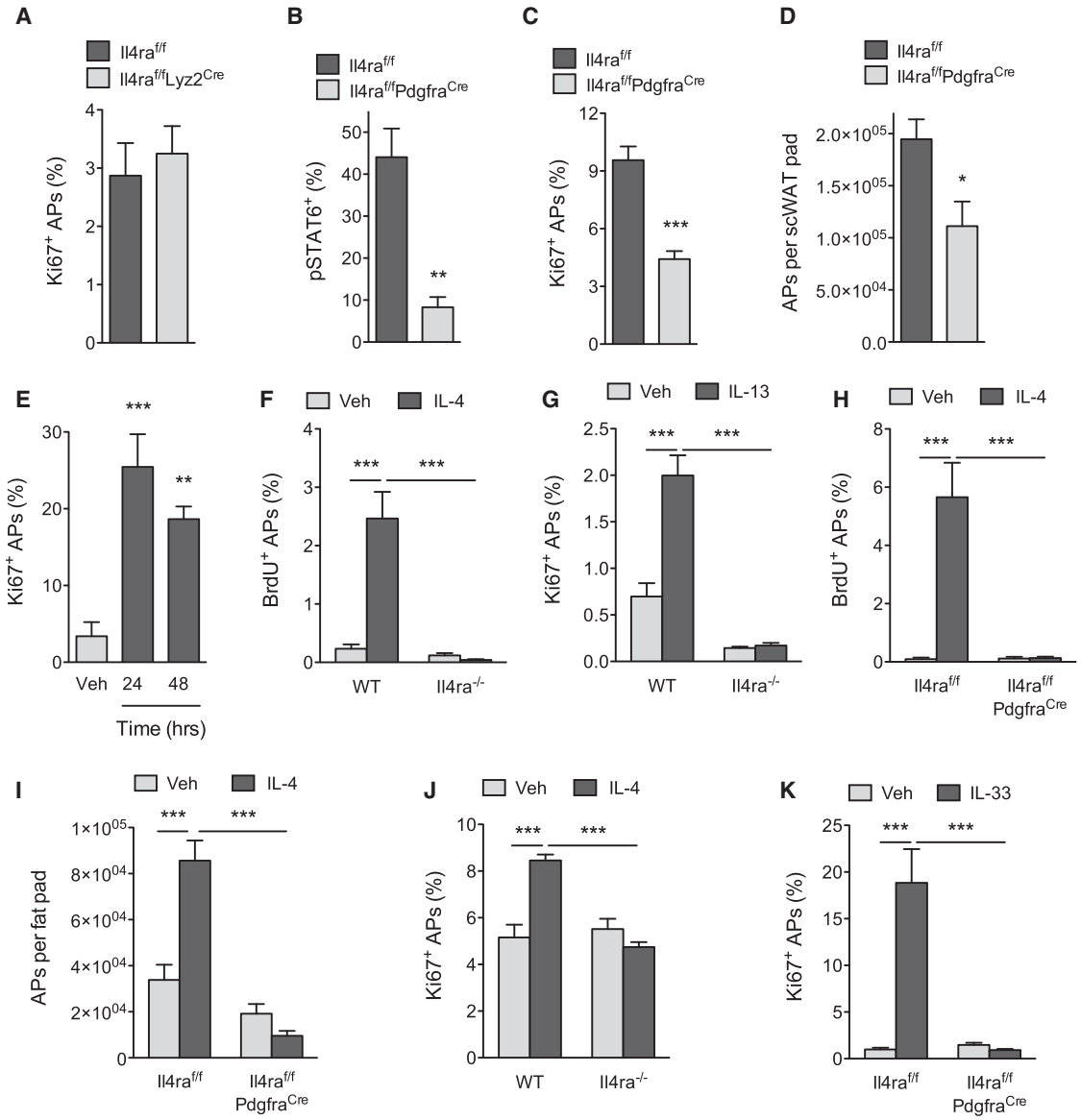

Figure 4. IL-4Rα Signaling in PDGFRα$^+$ Cells Promotes Expansion of Adipocyte Precursors

(A) Quantification of scWAT adipocyte precursor (AP) proliferation in 5-week-old *Il4ra*$^{f/f}$ and *Il4ra*$^{f/f}$/*Lyz2*^{Cre} mice (n = 8–10 per genotype).

(B) Analysis of IL-4-induced phosphorylation of STAT6 (pSTAT6) in scWAT APs of *Il4ra*$^{f/f}$ and *Il4ra*$^{f/f}$/*Pdgfra*^{Cre} mice (n = 3–4 per genotype).

(C and D) Quantification of scWAT AP proliferation by Ki67 staining (C) and total number (D) in 5-week-old *Il4ra*$^{f/f}$ and *Il4ra*$^{f/f}$/*Pdgfra*^{Cre} mice (n = 7–12). (E) Quantification of scWAT AP proliferation by Ki67 staining in 8- to 10-week-old C57BL/6J mice at 24 and 48 hr after injection with vehicle or IL-4 (n = 5 per time point).

(F and H) BrdU incorporation by the scWAT APs of wild-type and *Il4ra*$^{-/-}$ mice (F) or *Il4ra*$^{f/f}$ and *Il4ra*$^{f/f}$/*Pdgfra*^{Cre} mice (H) 48 hr after administration of IL-4 (n = 6–8 per genotype and treatment).

(G) Quantification of scWAT AP proliferation by Ki67 staining 48 hr after administration of vehicle or IL-13 (n = 6–8 per genotype and treatment).

(I) Quantification of scWAT AP number in *Il4ra*$^{f/f}$ and *Il4ra*$^{f/f}$/*Pdgfra*^{Cre} mice 48 hr after administration of vehicle or IL-4 (n = 7 per genotype).

(J) APs purified from wild-type and *Il4ra*$^{-/-}$ mice were stimulated with IL-4, and cellular proliferation was quantified by intracellular staining for Ki67 48 hr later (n = 4 per genotype and treatment).

(K) Quantification of scWAT AP proliferation in *Il4ra*$^{f/f}$ and *Il4ra*$^{f/f}$/*Pdgfra*^{Cre} mice 48 hr after administration of vehicle or IL-33 (n = 8–10 per genotype and treatment). Data are represented as mean ± SEM.

See also Figure S4.

myeloid cells, as in *Il4ra*$^{f/f}$*Lyz2*^{Cre} mice, did not significantly affect the rate of AP proliferation or expression of beige adipocyte markers in the scWAT (Figures 4A, S4A, and S4B), leading us to hypothesize that IL-4/13 might directly stimulate AP proliferation. To address this possibility, we generated mice in which *Il4ra* was selectively deleted in PDGFRα$^+$ cells (*Il4ra*$^{f/f}$*Pdgfra*^{Cre}

mice). Consistent with the loss of IL-4Rα expression in APs (Figure S4C), IL-4 stimulated increase in pSTAT6 was reduced by ~80% in scWAT APs, but not in the CD11b$^+$ myeloid cells, of *Il4ra*$^{f/f}$*Pdgfra*^{Cre} mice (Figures 4B, S4D, and S4E). Consequently, both the proliferative capacity of APs and their numbers were reduced by ~54% and ~43%, respectively, in 5-week-old *Il4ra*$^{f/f}$*Pdgfra*^{Cre} mice (Figures 4C and 4D). These results indicate that the type 2 cytokines IL-4 and IL-13 play a critical role in controlling adipocyte precursor pool size by directly activating IL-4Rα signaling in PDGFRα$^+$ APs.

To investigate whether pharmacological activation of IL-4Rα signaling is sufficient to stimulate the proliferation of APs in scWAT, we injected 8- to 10-week-old mice with IL-4 as a complex with anti-IL4 antibody, which prolongs its biological half-life (Finkelman et al., 1993). As noted above, the rate of AP proliferation declines with age (Figures 3A and 3B); however, this was restored by the administration of IL-4 to WT mice. For instance, treatment of 8- to 10-week-old mice with IL-4 complex increased the percentage of Ki67$^+$ APs by ~5.5–7.5-fold within 24–48 hr (Figure 4E). This stimulation of AP proliferation by IL-4 or IL-13 was an on-target effect of these cytokines because it required IL-4Rα (Figures 4F and 4G). Furthermore, administration of IL-4 complex failed to stimulate DNA synthesis or cellular proliferation in APs of *Il4ra*$^{f/f}$*Pdgfra*^{Cre} mice (Figures 4H and S4F), confirming that IL-4 stimulates the growth of APs in a cell autonomous manner. After 48 hr, the number of APs present in scWAT also increased by ~2.5-fold, demonstrating that stimulation with IL-4 is sufficient to expand the pool of PDGFRα$^+$ APs that reside within scWAT (Figures 4I and S4G). Again, this increase in AP number was dependent on cell autonomous signaling via the IL-4Rα in PDGFRα$^+$ cells (Figure 4I). Purification of APs from wild-type, *Il4ra*$^{-/-}$, and *Stat6*$^{-/-}$ mice provided independent verification for the direct proliferative effects of IL-4 on APs (Figures S4H, S4I, and 4J). Finally, we tested whether IL-33-induced proliferation of APs requires cell autonomous signaling via the IL-4Rα. Indeed, while IL-33 robustly induced AP proliferation (~19-fold) in the scWAT of *Il4ra*$^{f/f}$ mice, it failed to do so in *Il4ra*$^{f/f}$*Pdgfra*^{Cre} mice (Figure 4K). In a similar manner, the induction of IL-4Rα and beige adipocyte markers (TMEM26 and CD137) by IL-33 was absent in *Il4ra*$^{f/f}$*Pdgfra*^{Cre} mice (Figures S4J–S4L). In aggregate, these results demonstrate that the IL-33/ILC2/IL-4Rα signaling pathway acts directly on scWAT APs to expand the pool of beige adipogenic precursors.

IL-4 and IL-13 Direct Commitment of PDGFRα$^+$ Adipocyte Precursors to Beige Adipogenic Precursors

PDGFRα$^+$ APs present in scWAT are bipotential cells that can give rise to white or beige adipocytes (Berry et al., 2014; Lee et al., 2012), prompting us to ask whether signaling via the IL-4Rα might direct the commitment of APs to either lineage. Using purified wild-type APs from the scWAT, we first investigated the effects of IL-4 on their adipogenic conversion into white adipocytes. Figures S5A–S5C show that the addition of IL-4 during the initial differentiation period inhibited the conversion of APs into white adipocytes. Since differentiated adipocytes did not express IL-4Rα at any appreciable level (Figure S5C), we hypothesized that the biologic actions of type 2 cytokines might be restricted to adipogenic precursors. We thus asked whether, in the absence of adipogenic stimuli, treatment with IL-4 altered the fate of purified APs. Indeed, in a time-dependent manner, treatment of purified APs with IL-4 induced the expression of a number of beige adipocyte makers, including *Klhl13*, *Ear2*, *Tmem26*, and *Tnfrsf9* (Figure 5A). Consistent with the distinct developmental lineages of beige and brown adipocytes (Harms and Seale, 2013), exposure to IL-4 did not alter the expression of brown fat markers in APs purified from scWAT (Figure S5D). This commitment of APs to the beige fat lineage was an on-target effect of IL-4 because it was absent in APs isolated from *Il4ra*$^{-/-}$ mice (Figure 5B).

We next asked whether administration of IL-4 to wild-type mice was sufficient to promote the expression of beige lineage markers in APs. Cell surface expression of IL-4Rα, a known target of IL-4/STAT6 signaling (Goenka and Kaplan, 2011), and the beige precursor markers CD137 (encoded by *Tnfrsf9*) and TMEM26 were all induced in the scWAT APs upon treatment with IL-4 (Figures 5C–5H). The induction of these beige markers required intact IL-4Rα signaling in PDGFRα$^+$ cells because treatment with IL-4 failed to induce expression of CD137 and TMEM26 in scWAT APs of *Il4ra*$^{f/f}$*Pdgfra*^{Cre} mice (Figures 5I and 5J). Furthermore, treatment of WT mice with IL-4 was also sufficient to increase expression of beige cell markers in eWAT (Figures S6A–S6F), a tissue that is normally refractory to cold-induced browning. Consistent with these gain-of-function studies, loss of type 2 cytokine signaling, as in ΔdblGATA, *Il4/13*$^{-/-}$, and *Il4ra*$^{f/f}$*Pdgfra*^{Cre} mice, decreased expression of beige precursor cell markers in scWAT APs (Figures S6G–S6J and Figures 5K and 5L).

To investigate whether the induction of beige precursor cell markers correlates with enhanced capacity for beige adipogenesis, we pretreated purified APs with IL-4 and then subjected them to beige adipogenic stimuli. Congruent with our hypothesis, we observed that IL-4 pretreated APs exhibited enhanced capacity for beige adipogenesis, as assessed by the expression of UCP1 mRNA and protein (Figures 5M and 5N). Moreover, we observed that differentiation of APs into beige adipocytes resulted in downregulation of beige adipocyte markers (*Tnfrsf9, Klhl13*, and *Tmem26*) (Figure S6K), indicating that these markers might work better for the identification of beige adipocyte precursors rather than the differentiated beige adipocytes in WATs. Together, these in vitro and in vivo data suggest that the activation of signaling via the IL-4Rα in PDGFRα$^+$ cells is both required and sufficient to promote the commitment of bipotential APs to the beige fat lineage.

IL-4Rα Signaling in Adipocyte Precursors Controls Growth of Beige Fat

We next asked whether loss of IL-4Rα signaling in PDGFRα$^+$ cells alters the development of beige fat in vivo. The browning of scWAT normally occurs when mice experience cold stress. Since the standard vivarium temperature of 20°C–22°C poses a significant thermal stress for young mice (Cannon and Nedergaard, 2011; Nedergaard and Cannon, 2014), due to their high ratio of body surface area to body mass, we asked whether young (5-week-old) mice exhibited browning of their scWAT. We chose this time point because it represents the peak for scWAT AP IL-4Rα signaling and proliferation (Figures 3 and 4). Indeed, we found histological evidence for beige fat

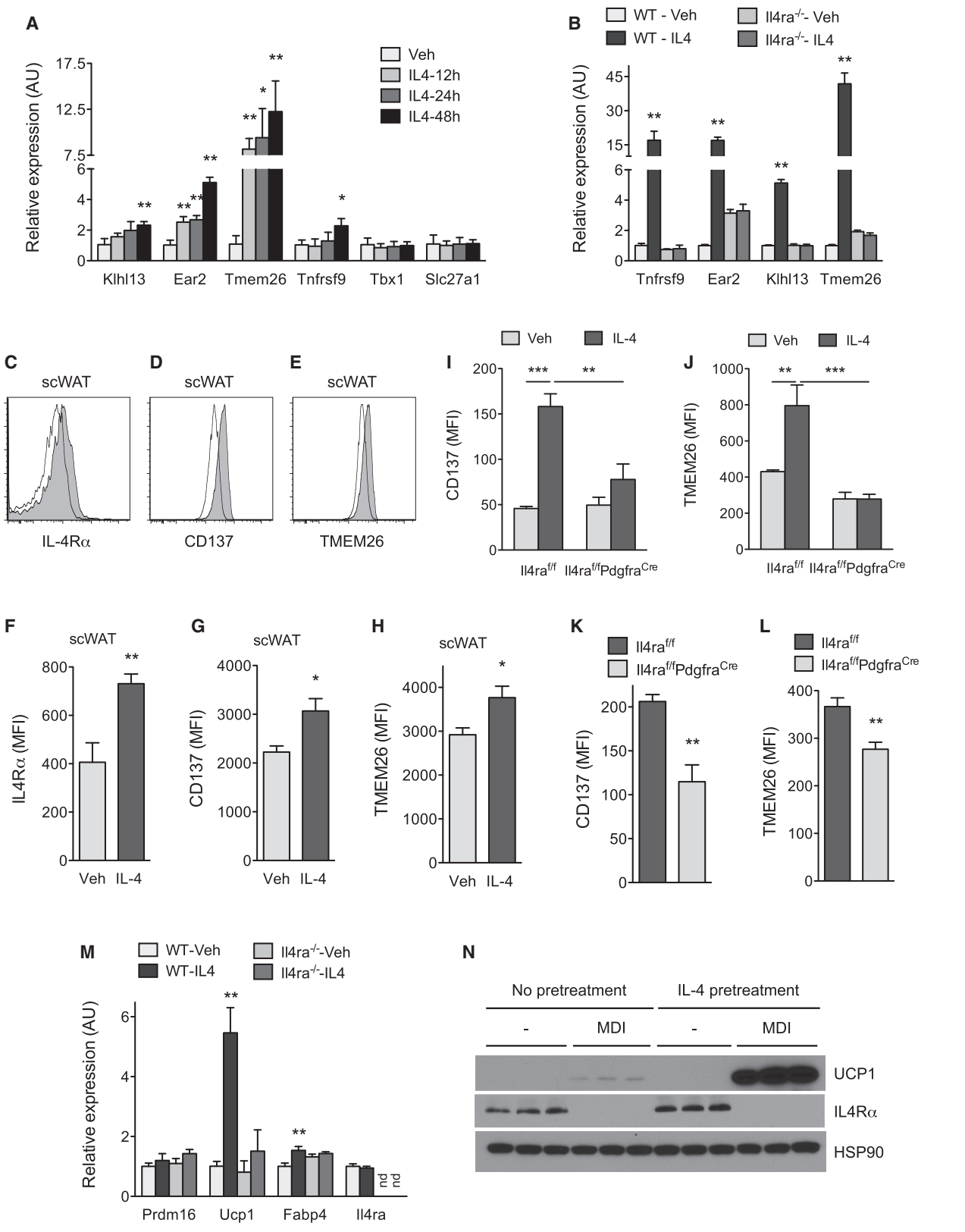

(legend on next page)

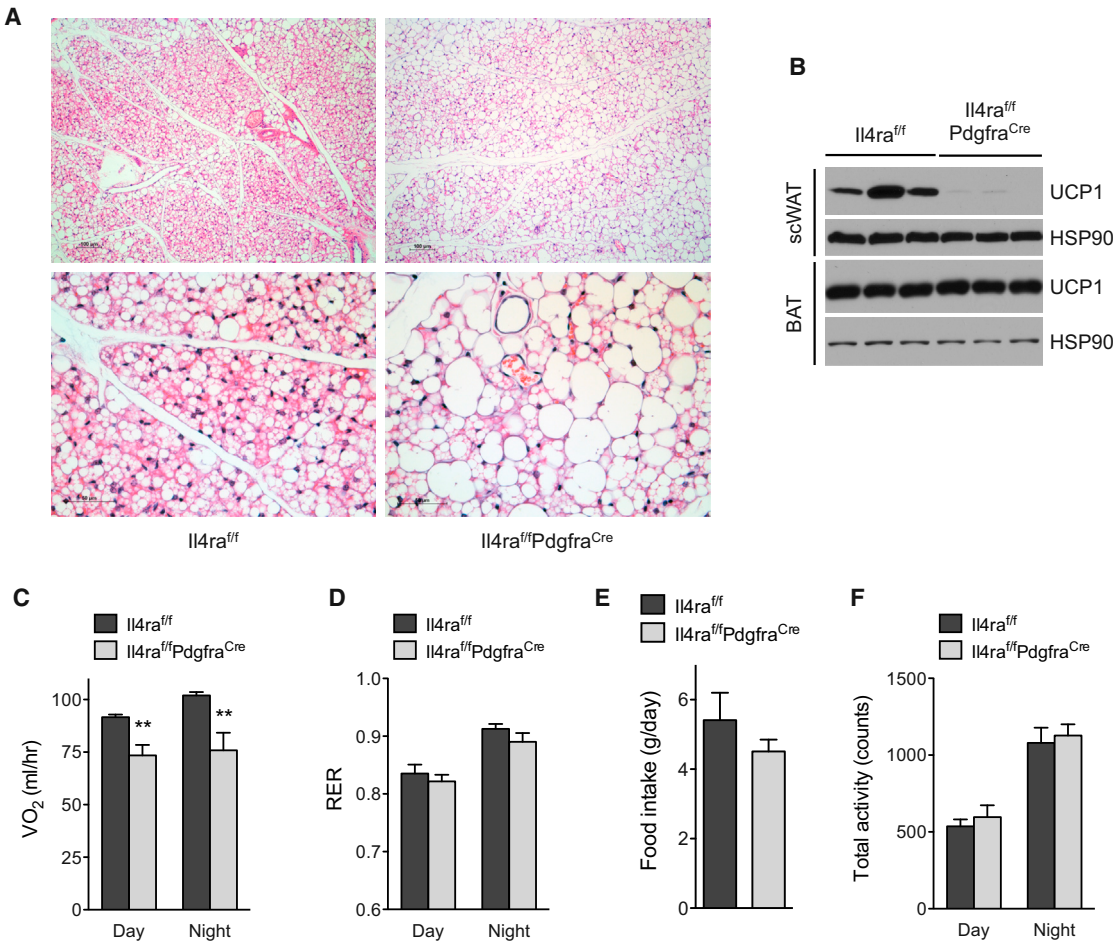

Figure 6. IL-4Rα Signaling in Adipocyte Precursors Directs Growth of Beige Fat

(A) Representative sections of scWAT from 5-week-old *Il4ra*$^{f/f}$ and *Il4ra*$^{f/f}$/*Pdgfra*^{Cre} mice were stained with hematoxylin and eosin. 100x magnification (top), 400x magnification (bottom). (B) UCP1 protein expression in scWAT and BAT of 5-week-old *Il4ra*$^{f/f}$ and *Il4ra*$^{f/f}$/*Pdgfra*^{Cre} mice housed at 22°C (n = 3 per genotype). (C–F) Assessment of metabolic rate, food intake, and activity in 5-week-old *Il4ra*$^{f/f}$ and *Il4ra*$^{f/f}$/*Pdgfra*^{Cre} mice housed at 22°C (n = 8 per genotype); (C) oxygen consumption (VO_2), (D) RER, (E) total activity, and (F) food intake. Data are represented as mean ± SEM.

development in the scWAT of control (*Il4ra*$^{f/f}$) mice housed at 20°C–22°C, which was decreased in the *Il4ra*$^{f/f}$*Pdgfra*^{Cre} mice (Figure 6A). Specifically, *Il4ra*$^{f/f}$ mice demonstrated complete replacement of multiple adjacent central scWAT lobules with multiloculated beige adipocytes, while beiging in *Il4ra*$^{f/f}$ *Pdgfra*^{Cre} mice, in contrast, involved fewer scWAT lobules, each of which exhibited less complete beiging (i.e., retained more cells with white adipocyte morphology). In agreement

Figure 5. IL-4 and IL-13 Direct Commitment of PDGFRα^{+} Adipocyte Precursors to Beige Adipogenic Precursors

(A) Quantitative RT-PCR analysis of beige adipocyte precursor markers in APs purified from the scWAT of C57BL/6J stimulated with vehicle or IL-4 (n = 3 per condition and time point; data presented as mean ± SD).

(B) Quantitative RT-PCR analysis of beige adipocyte precursor markers in APs purified from Balb/cJ or *Il4ra*$^{-/-}$ mice that were stimulated with vehicle or IL-4 for 48 hr (n = 3 per genotype and treatment; data presented as mean ± SD).

(C–E) Flow cytometric analysis of IL-4Rα (C), CD137 (D) and TMEM26 (E) expression in scWAT APs of mice injected with vehicle or IL-4. Clear histogram: vehicle; shaded histogram: IL-4.

(F–H) Quantification of IL-4Rα, CD137, and TMEM26 expression in scWAT APs 48 hr after administration of vehicle or IL-4 (n = 5 per treatment). (I, J) Quantification of CD137 and TMEM26 expression in the scWAT APs of *Il4ra*$^{f/f}$ and *Il4ra*$^{f/f}$/*Pdgfra*^{Cre} mice 48 hr after administration of IL-4 (n = 4–6 per genotype and treatment). (K and L) Quantification of CD137 and TMEM26 expression in the scWAT APs of 5-week-old *Il4ra*$^{f/f}$ and *Il4ra*$^{f/f}$/*Pdgfra*^{Cre} mice (n = 8–12 per genotype).

(M) Quantitative RT-PCR analysis of beige/brown adipocyte genes after in vitro differentiation of scWAT APs purified from Balb/cJ or *Il4ra*$^{-/-}$ mice (n = 3 per genotype and treatment; data presented as mean ± SD).

(N) Immunoblot analysis for UCP1 and IL-4Rα in in vitro-differentiated APs. MDI refers to stimulation of differentiation by adipogenic cocktail, (n = 3 genotype and treatment).

Unless otherwise indicated, data are represented as mean ± SEM. See also Figure S5 and S6.

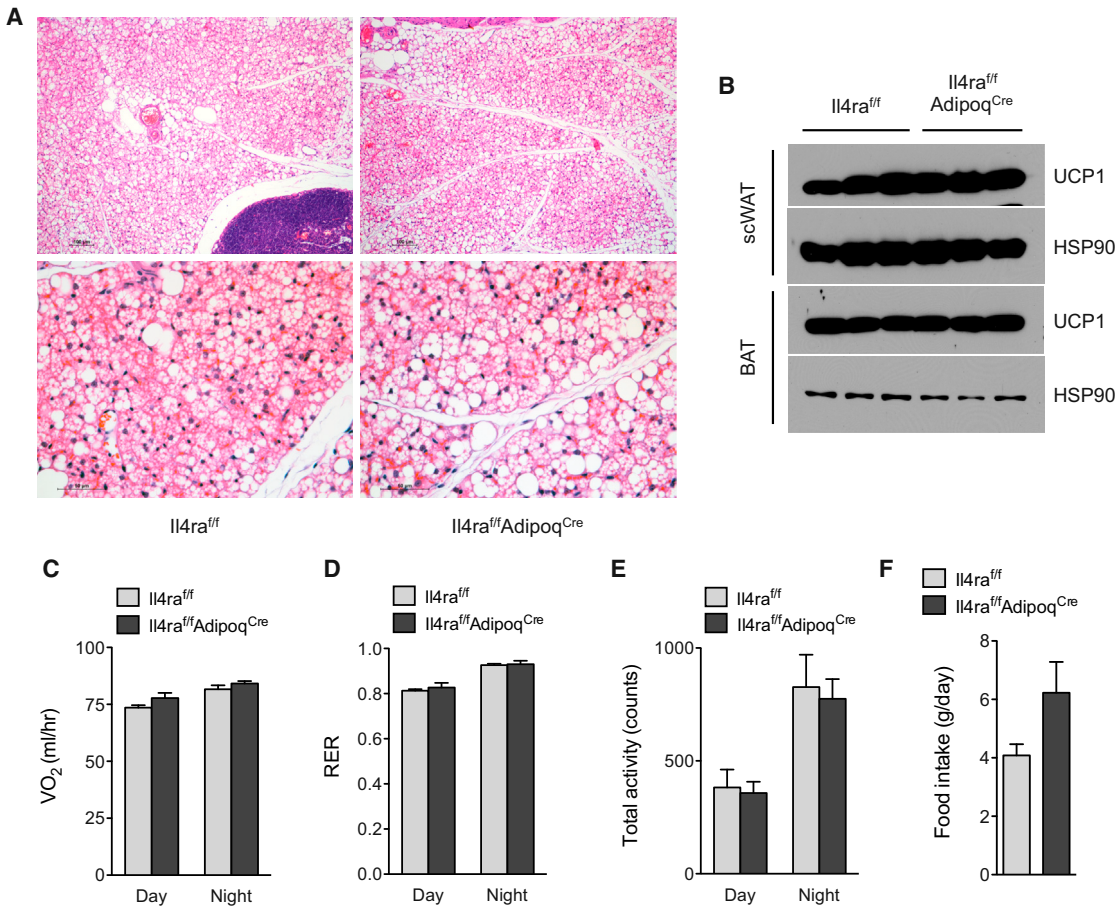

Figure 7. IL-4Rα Signaling in Mature Adipocytes Is Dispensable for Growth of Beige Fat

(A) Histological analysis of scWAT of 5-week-old *Il4ra*$^{f/f}$ and *Il4ra*$^{f/f}$/*Adipoq*^{Cre} mice housed at 22°C. Representative sections were stained with hematoxylin and eosin, and images are shown at 100× magnification (top) and 400× magnification (bottom).

(B) Immunoblot analysis of UCP1 protein expression in scWAT and BAT of 5-week-old *Il4ra*$^{f/f}$ and *Il4ra*$^{f/f}$/*Adipoq*^{Cre} mice.

(C–F) Assessment of energy expenditure in 5-week-old *Il4ra*$^{f/f}$ and *Il4ra*$^{f/f}$/*Adipoq*^{Cre} mice was performed using CLAMS; (C) oxygen consumption (VO_2), (D) RER, (E) total activity, and (F) food intake. Data are represented as mean ± SEM.

with these histological data, immunoblot analysis for UCP1 protein demonstrated its robust expression in the scWAT of *Il4ra*$^{f/f}$ but not *Il4ra*$^{f/f}$*Pdgfra*^{Cre} mice (Figure 6B). In contrast, we did not observe significant differences among the genotypes in expression of UCP1 protein in interscapular brown adipose tissue (Figure 6B), which develops from distinct myogenic precursors (Lepper and Fan, 2010; Seale et al., 2008).

To investigate whether browning of scWAT in young mice contributed to total body energy expenditure, we studied 5-week-old mice *Il4ra*$^{f/f}$ and *Il4ra*$^{f/f}$*Pdgfra*^{Cre} mice using the Comprehensive Lab Animal Monitoring Systems (CLAMS). Energy expenditure, as quantified by total oxygen consumption (VO_2) per mouse, was significantly lower (~20%–25%) in *Il4ra*$^{f/f}$*Pdgfra*^{Cre} mice in both the day and night cycle (Figure 6C). This reduction in VO2 was unlikely to be a consequence of changes in total locomotor activity, RER, or food intake, which were similar between the two genotypes (Figure 6D–6F). Together, these results demonstrate that IL-4Rα signaling in adipocyte precursor cells is a critical regulator for the development of postnatal beige fat.

IL-4Rα Signaling in Mature Adipocytes Is Dispensable for Growth of Beige Fat

Because adipogenic precursors give rise to mature adipocytes (Berry et al., 2014), it remains plausible that the metabolic phenotypes observed in *Il4ra*$^{f/f}$*Pdgfra*^{Cre} mice result from loss of IL-4Rα signaling in mature adipocytes. To address this possibility, we generated mice in which the *Il4ra* gene was selectively deleted in differentiated adipocytes (designated *Il4ra*$^{f/f}$*Adipoq*^{Cre}). Consistent with its primary role in APs, deletion of *Il4ra* in mature adipocytes did not affect beige fat development as assessed histologically and by immunoblotting for UCP1 (Figures 7A, 7B and S6L). Accordingly, *Il4ra*$^{f/f}$ and *Il4ra*$^{f/f}$*Adipoq*^{Cre} mice had similar rates of oxygen consumption, RER, total activity, and food intake (Figures 7C–7F). These findings are consistent with the observations that IL-4Rα is highly expressed in adipogenic

precursors but not in mature adipocytes (Figures 5N and S5C).

DISCUSSION

We have previously demonstrated that exposure to environmental cold induces an innate type 2 response to stimulate the growth of beige fat. This efferent innate circuit consists of IL-4-secreting eosinophils and catecholamine-producing alternatively activated macrophages (Nguyen et al., 2011; Qiu et al., 2014). Here we have identified two additional components of this thermogenic circuit, which include ILC2s and PDGFRα$^+$ adipogenic precursors. Using IL-33 to pharmacologically activate ILC2s in thermoneutral mice, we were able to place ILC2s upstream of APs in the beige fat thermogenic circuit. We found that ILC2-derived IL-13 and eosinophil-derived IL-4 functionally cooperate to activate IL-4Rα signaling, thus promoting the expansion and commitment of scWAT APs to the beige adipocyte lineage. Surprisingly, these browning effects of IL-4 and IL-13 were not dependent on signaling via the IL-4Rα on myeloid cells but rather on PDGFRα$^+$ APs themselves. In agreement with this, both pharmacologic and physiologic expansion of beige adipocyte precursors was reduced in *Il4ra*$^{f/f}$*Pdgfra*^{Cre} mice. Taken together with our previous results, these findings suggest that type 2 immunity regulates two key events in the biogenesis of beige fat. First, it controls the expansion and commitment of APs to the beige fat lineage. Second, it stimulates the differentiation of beige precursor cells into beige adipocytes via myeloid cell-derived catecholamines.

Browning of WAT has principally been studied in adult rodents after prolonged exposure to cold (Nedergaard and Cannon, 2014; Wu et al., 2013). In these experimental paradigms, the housing of adult mice in cold environments (4°C–8°C for 2 days or longer) promotes the emergence of UCP1$^+$ multilocular beige adipocytes. The underlying assumption here has been that prolonged cold exposure creates a mismatch between the organism's capacity for heat generation and its heat loss to the environment, necessitating the recruitment of additional thermogenic tissues to maintain thermal homeostasis (Nedergaard and Cannon, 2014; Qiu et al., 2014). Because the normal vivarium temperature of 20°C–22°C imposes a significant thermal stress on young mice, in which the ratio of body surface area to body mass is large, we reasoned that it might be a powerful stimulus for the recruitment of UCP1$^+$ beige adipocytes. Indeed, we found histological evidence for browning in the scWAT of 5-week-old mice housed at 20°C–22°C. Unlike the cold-induced browning in adult mice, which is generally patchy and incomplete even within individual lobules, this "physiologic" browning of the scWAT in young mice was more widespread, involving entire adjacent lobules (Figures 6A and 7A). Thus, we suggest that, as an alternative to the classic experimental paradigm of housing adult mice at 4°C–8°C, investigations of the physiologic browning process in young mice might yield useful insights into the mechanisms that regulate beige fat biogenesis.

Although the stages of scWAT development have been studied previously (Wang et al., 2013), the physiologic signals that regulate the proliferation and/or fate of scWAT APs were unknown. Our observations that IL-33 potently stimulates proliferation of PDGFRα$^+$ APs in an IL-4/13- and IL-4Rα-dependent manner (Figures 2K and 2L) led us to investigate whether type 2 cytokines might be the physiologic signals controlling the expansion of PDGFRα$^+$ APs in the scWAT. Indeed, we found that loss of type 2 cytokine signaling decreased the proliferation rate and number of PDGFRα$^+$ APs by ~50% in scWAT. Interestingly, this signaling pathway also regulated the commitment of PDGFRα$^+$ APs to the beige adipocyte precursors in a cell autonomous manner. Since the proliferation rate of PDGFRα$^+$ APs declines with age (Figures 3A and 3B), our results suggest that the activation of type 2 cytokine signaling in the early postnatal period establishes a pool of PDGFRα$^+$ beige adipocyte precursors, which are subsequently recruited by cold stress to generate beige adipocytes in the adult organism. Perhaps, these data also provide an explanation for the old observation that thermogenic adaptations to cold decline with aging (Talan et al., 1985).

Our gain- and loss-of-function studies suggest that type 2 innate immune cells have discrete roles in controlling the numbers and fate of PDGFRα$^+$ adipocyte precursors in the scWAT of mice. During physiologic development of this tissue, eosinophil-derived IL-4 seems to play a critical role in the homeostatic expansion of PDGFRα$^+$ APs into beige adipocyte precursors in young mice (Figures 3E, 3F, S6G, and S6H). However, IL-33-induced pharmacologic expansion of scWAT APs in adult animals seems to occur independently of eosinophils (Figure S2H). Since both ILC2s and signaling via the IL-4Rα are required for IL-33-mediated proliferation of scWAT APs and their subsequent differentiation into beige adipocytes (Figures 2K–2P), it suggests that secretion of IL-13 by ILC2s might be a dominant mechanism by which this tissue responds to environmental stress. Thus, in the future, it will be critical to examine the requirement of and mechanisms by which ILC2s and IL-33 regulate the development of functional beige fat during cold stress.

Finally, together with previous studies, our work provides mechanistic insights into how mammals adapt and acclimatize to environmental cold. During an acute cold challenge, mice defend their core body temperature by quickly activating thermogenesis. This rapid increase in heat production, which occurs within seconds to minutes, is mediated by several thermoeffectors, including cutaneous vasoconstriction, skeletal muscle shivering, and UCP1-mediated respiration in brown adipocytes; processes that are all activated by the sympathetic nervous system (Cannon and Nedergaard, 2011; Lowell and Spiegelman, 2000). In contrast, prolonged cold stress induces cellular programs for acclimatization, such as the de novo recruitment of beige adipocytes (Harms and Seale, 2013), which occur on a longer time frame (days to weeks to months) for more stable physiologic adaptations. Although programs of acclimatization are well documented across species and are of great interest to evolutionary biologists, their mechanisms, with a few exceptions (such as changes in skin pigmentation in response to sunlight or increase in oxygen carrying capacity after living at high altitudes), are largely unknown. Through our work, we have identified the mechanism for acclimatization to environmental cold. Unlike the acute adaptations that are initiated by the sympathetic nervous system, acclimatization to environmental cold is orchestrated by type 2 immune cells (ILC2s, eosinophils, and

alternatively activated macrophages) and signals (IL-33, IL-4, and -13), which sequentially regulate the expansion, commitment, and differentiation of adipocyte precursors into beige adipocytes. Our identification of the immune system as the primary thermogenic circuit controlling the cold acclimatization process is consistent with a recent proposal that type 2 immunity coevolved as a defensive strategy against noxious environmental stimuli (Palm et al., 2012; Profet, 1991), of which cold might be one.

EXPERIMENTAL PROCEDURES

Animal Studies

All animal studies were conducted at UCSF under an approved IACUC protocol. Mice were housed at 20°C–22°C (unless otherwise stated) in the vivarium under a 12 hr light:dark cycle. Both male and female mice of various ages were used in these studies. The following animal strains were on the BALB/cJ background: WT, *Il4/13*$^{-/-}$, *Il4ra*$^{-/-}$, *Stat6*$^{-/-}$, *4get*, and 4get-ΔdblGATA, whereas WT, R5 (*Il5*$^{Red5/+}$), R5R5 (*Il5*$^{Red5/Red5}$), R5Smart13 (*Il5*$^{Red5/+}$*Il13*$^{Smart/+}$), *Il4ra*$^{-/-}$, *Ucp1*$^{-/-}$, *Il4ra*$^{f/f}$, *Il4ra*$^{f/f}$*Lyz2*^{Cre}, *Il4ra*$^{f/f}$*Pdgfra*^{Cre}, and *Il4ra*$^{f/f}$*Adipoq*^{Cre} were on the C57BL6/J background. *Rag2*$^{-/-}$ and *Rag2Il2rg*$^{-/-}$ were purchased from Taconic. At the conclusion of experiments, tissues were harvested and snap frozen in liquid nitrogen for molecular analyses, fixed in 10% formalin for histology, or digested for flow cytometric analyses of adipocyte precursors and immune cells. For gain-of-function studies, 8- to 12-week-old mice were injected intraperitoneally with vehicle, IL-33 (0.5–1 μg, Biolegend), IL-13 (0.5 μg, Peprotech), or IL-4 (2 μg, Peprotech) that was complexed with anti-IL4 mAb (10 μg, clone 11B11). Activation of signaling via the IL-4Rα was assessed 1–2 hr after administration of recombinant IL-4 (2 μg). For the in vivo studies, cohorts of ≥4 mice per genotype or treatment were assembled and experiments were repeated 2–3 independent times.

Statistical Analysis

Data were analyzed using Prism (Graphpad) and are presented as mean ± SEM or mean ± SD. Statistical significance was determined using the unpaired two-tailed Student's t test for single variables and two-way ANOVA followed by Bonferroni posttests for multiple variables. A p value of < 0.05 was considered to be statistically significant and is presented as * ($p < 0.05$), ** ($p < 0.01$), or *** ($p < 0.001$).

Extended Experimental Procedures are included in the Supplemental Information.

SUPPLEMENTAL INFORMATION

Supplemental Information includes Extended Experimental Procedures, seven figures, and two tables and can be found with this article online at http://dx.doi.org/10.1016/j.cell.2014.12.011.

AUTHOR CONTRIBUTION

M-W.L., J.I.O., L.M., Y.Q., A.B.M., and J.C.N. designed and performed the main experiments, and K.Y. provided technical assistance for the main experiments. R.M.L. provided essential mouse lines for the completion of the studies and assisted with experimental design and manuscript preparation. M-W.L., J.I.O., L.M., Y.Q., A.B.M, J.C.N., R.M.L., and A.C. discussed and interpreted the results from the study. M-W.L., J.I.O., and A.C. conceived, supervised, and wrote the paper.

ACKNOWLEDGMENTS

We thank members of the Chawla laboratory and A. Loh for comments on the manuscript. The authors' work was supported by grants from NIH (HL076746, DK094641), American Heart Association Innovative Science Award (12PILT11840038 and 14ISA20850001), an NIH Director's Pioneer Award (DP1AR064158) to A.C. and NIH (R37AI026918, AI119944) and HHMI to R.M.L. M-W.L. was supported by a Postdoctoral Fellowship from the Hillblom Foundation, A.B.M. by NIH K08 DK101604, and J.C.N. by NIH K08 AI113143.

Received: November 10, 2014
Revised: December 3, 2014
Accepted: December 3, 2014
Published: December 24, 2014

REFERENCES

Berry, R., and Rodeheffer, M.S. (2013). Characterization of the adipocyte cellular lineage in vivo. Nat. Cell Biol. *15*, 302–308.

Berry, R., Jeffery, E., and Rodeheffer, M.S. (2014). Weighing in on adipocyte precursors. Cell Metab. *19*, 8–20.

Cannon, B., and Nedergaard, J. (2011). Nonshivering thermogenesis and its adequate measurement in metabolic studies. J. Exp. Biol. *214*, 242–253.

Cayrol, C., and Girard, J.P. (2014). IL-33: an alarmin cytokine with crucial roles in innate immunity, inflammation and allergy. Curr. Opin. Immunol. *31C*, 31–37.

Finkelman, F.D., Madden, K.B., Morris, S.C., Holmes, J.M., Boiani, N., Katona, I.M., and Maliszewski, C.R. (1993). Anti-cytokine antibodies as carrier proteins. Prolongation of in vivo effects of exogenous cytokines by injection of cytokine-anti-cytokine antibody complexes. J. Immunol. *151*, 1235–1244.

Goenka, S., and Kaplan, M.H. (2011). Transcriptional regulation by STAT6. Immunol. Res. *50*, 87–96.

Golozoubova, V., Cannon, B., and Nedergaard, J. (2006). UCP1 is essential for adaptive adrenergic nonshivering thermogenesis. Am. J. Physiol. Endocrinol. Metab. *291*, E350–E357.

Harms, M., and Seale, P. (2013). Brown and beige fat: development, function and therapeutic potential. Nat. Med. *19*, 1252–1263.

Hudak, C.S., Gulyaeva, O., Wang, Y., Park, S.M., Lee, L., Kang, C., and Sul, H.S. (2014). Pref-1 marks very early mesenchymal precursors required for adipose tissue development and expansion. Cell Rep *8*, 678–687.

Kelly-Welch, A.E., Hanson, E.M., Boothby, M.R., and Keegan, A.D. (2003). Interleukin-4 and interleukin-13 signaling connections maps. Science *300*, 1527–1528.

Koyasu, S., and Moro, K. (2013). Th2-type innate immune responses mediated by natural helper cells. Ann. N Y Acad. Sci. *1283*, 43–49.

Lee, Y.H., Petkova, A.P., Mottillo, E.P., and Granneman, J.G. (2012). In vivo identification of bipotential adipocyte progenitors recruited by β3-adrenoceptor activation and high-fat feeding. Cell Metab. *15*, 480–491.

Lepper, C., and Fan, C.M. (2010). Inducible lineage tracing of Pax7-descendant cells reveals embryonic origin of adult satellite cells. Genesis *48*, 424–436.

Licona-Limón, P., Kim, L.K., Palm, N.W., and Flavell, R.A. (2013). TH2, allergy and group 2 innate lymphoid cells. Nat. Immunol. *14*, 536–542.

Lowell, B.B., and Spiegelman, B.M. (2000). Towards a molecular understanding of adaptive thermogenesis. Nature *404*, 652–660.

McKenzie, A.N., Spits, H., and Eberl, G. (2014). Innate lymphoid cells in inflammation and immunity. Immunity *41*, 366–374.

Mohrs, M., Shinkai, K., Mohrs, K., and Locksley, R.M. (2001). Analysis of type 2 immunity in vivo with a bicistronic IL-4 reporter. Immunity *15*, 303–311.

Molofsky, A.B., Nussbaum, J.C., Liang, H.E., Van Dyken, S.J., Cheng, L.E., Mohapatra, A., Chawla, A., and Locksley, R.M. (2013). Innate lymphoid type 2 cells sustain visceral adipose tissue eosinophils and alternatively activated macrophages. J. Exp. Med. *210*, 535–549.

Moro, K., Yamada, T., Tanabe, M., Takeuchi, T., Ikawa, T., Kawamoto, H., Furusawa, J., Ohtani, M., Fujii, H., and Koyasu, S. (2010). Innate production of T(H) 2 cytokines by adipose tissue-associated c-Kit(+)Sca-1(+) lymphoid cells. Nature *463*, 540–544.

Nedergaard, J., and Cannon, B. (2014). The browning of white adipose tissue: some burning issues. Cell Metab. *20*, 396–407.

Neill, D.R., Wong, S.H., Bellosi, A., Flynn, R.J., Daly, M., Langford, T.K., Bucks, C., Kane, C.M., Fallon, P.G., Pannell, R., et al. (2010). Nuocytes represent a new innate effector leukocyte that mediates type-2 immunity. Nature *464*, 1367–1370.

Nguyen, K.D., Qiu, Y., Cui, X., Goh, Y.P., Mwangi, J., David, T., Mukundan, L., Brombacher, F., Locksley, R.M., and Chawla, A. (2011). Alternatively activated macrophages produce catecholamines to sustain adaptive thermogenesis. Nature *480*, 104–108.

Nussbaum, J.C., Van Dyken, S.J., von Moltke, J., Cheng, L.E., Mohapatra, A., Molofsky, A.B., Thornton, E.E., Krummel, M.F., Chawla, A., Liang, H.E., and Locksley, R.M. (2013). Type 2 innate lymphoid cells control eosinophil homeostasis. Nature *502*, 245–248.

Palm, N.W., Rosenstein, R.K., and Medzhitov, R. (2012). Allergic host defences. Nature *484*, 465–472.

Price, A.E., Liang, H.E., Sullivan, B.M., Reinhardt, R.L., Eisley, C.J., Erle, D.J., and Locksley, R.M. (2010). Systemically dispersed innate IL-13-expressing cells in type 2 immunity. Proc. Natl. Acad. Sci. USA *107*, 11489–11494.

Profet, M. (1991). The function of allergy: immunological defense against toxins. Q. Rev. Biol. *66*, 23–62.

Qiu, Y., Nguyen, K.D., Odegaard, J.I., Cui, X., Tian, X., Locksley, R.M., Palmiter, R.D., and Chawla, A. (2014). Eosinophils and type 2 cytokine signaling in macrophages orchestrate development of functional beige fat. Cell *157*, 1292–1308.

Rao, R.R., Long, J.Z., White, J.P., Svensson, K.J., Lou, J., Lokurkar, I., Jedrychowski, M.P., Ruas, J.L., Wrann, C.D., Lo, J.C., et al. (2014). Meteorin-like is a hormone that regulates immune-adipose interactions to increase beige fat thermogenesis. Cell *157*, 1279–1291.

Rosen, E.D., and Spiegelman, B.M. (2006). Adipocytes as regulators of energy balance and glucose homeostasis. Nature *444*, 847–853.

Rosen, E.D., and Spiegelman, B.M. (2014). What we talk about when we talk about fat. Cell *156*, 20–44.

Sanchez-Gurmaches, J., Hung, C.M., Sparks, C.A., Tang, Y., Li, H., and Guertin, D.A. (2012). PTEN loss in the Myf5 lineage redistributes body fat and reveals subsets of white adipocytes that arise from Myf5 precursors. Cell Metab. *16*, 348–362.

Seale, P., Bjork, B., Yang, W., Kajimura, S., Chin, S., Kuang, S., Scimè, A., Devarakonda, S., Conroe, H.M., Erdjument-Bromage, H., et al. (2008). PRDM16 controls a brown fat/skeletal muscle switch. Nature *454*, 961–967.

Talan, M.I., Engel, B.T., and Whitaker, J.R. (1985). A longitudinal study of tolerance to cold stress among C57BL/6J mice. J. Gerontol. *40*, 8–14.

van der Lans, A.A., Hoeks, J., Brans, B., Vijgen, G.H., Visser, M.G., Vosselman, M.J., Hansen, J., Jörgensen, J.A., Wu, J., Mottaghy, F.M., et al. (2013). Cold acclimation recruits human brown fat and increases nonshivering thermogenesis. J. Clin. Invest. *123*, 3395–3403.

Van Dyken, S.J., Mohapatra, A., Nussbaum, J.C., Molofsky, A.B., Thornton, E.E., Ziegler, S.F., McKenzie, A.N., Krummel, M.F., Liang, H.E., and Locksley, R.M. (2014). Chitin activates parallel immune modules that direct distinct inflammatory responses via innate lymphoid type 2 and $\gamma\delta$ T cells. Immunity *40*, 414–424.

Walker, J.A., Barlow, J.L., and McKenzie, A.N. (2013). Innate lymphoid cells—how did we miss them? Nat. Rev. Immunol. *13*, 75–87.

Wang, Q.A., Tao, C., Gupta, R.K., and Scherer, P.E. (2013). Tracking adipogenesis during white adipose tissue development, expansion and regeneration. Nat. Med. *19*, 1338–1344.

Wang, W., Kissig, M., Rajakumari, S., Huang, L., Lim, H.W., Won, K.J., and Seale, P. (2014). Ebf2 is a selective marker of brown and beige adipogenic precursor cells. Proc. Natl. Acad. Sci. USA *111*, 14466–14471.

Wu, D., Molofsky, A.B., Liang, H.E., Ricardo-Gonzalez, R.R., Jouihan, H.A., Bando, J.K., Chawla, A., and Locksley, R.M. (2011). Eosinophils sustain adipose alternatively activated macrophages associated with glucose homeostasis. Science *332*, 243–247.

Wu, J., Boström, P., Sparks, L.M., Ye, L., Choi, J.H., Giang, A.H., Khandekar, M., Virtanen, K.A., Nuutila, P., Schaart, G., et al. (2012). Beige adipocytes are a distinct type of thermogenic fat cell in mouse and human. Cell *150*, 366–376.

Wu, J., Cohen, P., and Spiegelman, B.M. (2013). Adaptive thermogenesis in adipocytes: is beige the new brown? Genes Dev. *27*, 234–250.

Yoneshiro, T., Aita, S., Matsushita, M., Kayahara, T., Kameya, T., Kawai, Y., Iwanaga, T., and Saito, M. (2013). Recruited brown adipose tissue as an antiobesity agent in humans. J. Clin. Invest. *123*, 3404–3408.

Yu, C., Cantor, A.B., Yang, H., Browne, C., Wells, R.A., Fujiwara, Y., and Orkin, S.H. (2002). Targeted deletion of a high-affinity GATA-binding site in the GATA-1 promoter leads to selective loss of the eosinophil lineage in vivo. J. Exp. Med. *195*, 1387–1395.

Zeve, D., Tang, W., and Graff, J. (2009). Fighting fat with fat: the expanding field of adipose stem cells. Cell Stem Cell *5*, 472–481.

Cell

EXTENDED EXPERIMENTAL PROCEDURES

Flow Cytometry

scWAT and eWAT were digested in 2 ml of Collagenase I buffer (2 $mgml^{-1}$ at 250U/mg, Worthington, and 30 $mgml^{-1}$ bovine serum albumin in Hams F-10 medium) at 37°C for 20–30 min. The homogenates were washed and filtered (40 μm) prior to immunostaining for flow cytometric analysis. Cell suspensions were stained with Zombie Aqua TM (1:1,000, Biolegend) in PBS containing EDTA (5 mM) for 15 min, washed, and then resuspended in FACS buffer (PBS, 5 mM EDTA, and 2.5% FBS). Cell suspensions were pre-incubated with Fc receptor block (0.5 μg) and then stained with the appropriate primary and secondary antibodies. Staining with lineage cocktail, which contains anti-CD3, -Ly-6G, -Ly-6C, -CD11b, -CD45R/B220, -Ter-119 (Biolegend, 1:200), was used to exclude other cell lineages from the analysis gates. For analyses of Ki67 and beige markers (CD137 and TMEM26) expression in adipocyte precursors, cells were fixed and permeabilized using the Fixation/Permeabilization kit (eBioscience) as per manufacturer's protocol. In some instances, CD137 and TMEM26 MFI were quantified by subtracting the MFI of controls stained without the specific primary antibody from samples stained with both primary and secondary antibodies. For analysis of pSTAT6, cells were stained for viability and CD31 and subsequently fixed in 1.6% paraformaldehyde for 30 min at 4°C. Fixed cells were permeabilized with 100% ice cold methanol for 30 min, washed extensively in FACS buffer to remove all traces of methanol, and stained with anti-pSTAT6 antibody. Antibody sources and dilutions are listed in Table S1. Data were acquired using FACSVerse (Becton Dickinson) and analyzed using FlowJo software.

BrdU Studies

To assess age-dependent proliferation of adipocyte precursors, mice were administered BrdU in drinking water (0.8 $mgml^{-1}$) for 2 weeks. To quantify IL-4-induced proliferation of adipocyte precursors, mice were injected with BrdU (100 $mgkg^{-1}$) 18 hr prior to collection of tissues. After digestion and staining for cellular viability, cellular suspensions were stained for CD31 and resuspended in Cytofix/Cytoperm™ (Becton Dickinson) for 30 min. The fixed cells were then permeabilized using Perm/Wash™ buffer (Becton Dickinson), treated with DNase 1 (Roche) for 1 hr at 37°C, and stained with antibodies directed against BrdU and appropriate lineage markers.

Quantitative RT-PCR

Total RNA was extracted from tissues homogenized in TRIsure (Bioline) reagent. Isolated RNA was reverse transcribed using qScript cDNA SuperMix (Quanta), and the resulting cDNA was used for quantitative PCR on a CFX384 real-time PCR detection system (Bio-Rad). Relative mRNA expression level was determined using the 2(-Delta Delta C(T)) method with 36B4 as the internal reference control. Primer sequences are listed in Table S2.

Immunoblotting

Snap-frozen tissues were homogenized in modified RIPA buffer (420 mM NaCl, 1% NP-40, 0.1% SDS, 0.5% sodium deoxycholate, 50 mM Tris pH 7.5, and protease inhibitor cocktail) using a TissueLyser II (QIAGEN). Total protein (30–50 μg) was separated by SDS–PAGE and electrophoretically transferred to nitrocellulose membranes, which were then blocked, probed with the primary and HRP-conjugated secondary antibodies (listed in Table S1), and developed with SuperSignal West Pico Chemiluminescent Substrate (Thermo Scientific).

Energy Expenditure

Energy expenditure and associated measurements were performed using a temperature-controlled CLAMS chamber (Columbus Instruments) according to the manufacturer's protocols. Briefly, mice were acclimatized to chambers for 2 days prior to data collection, after which metabolic data were collected across different ambient temperatures ranging from 30°C to 5°C. Oxygen consumption rate (VO_2) and CO_2 release rates (VCO_2) were monitored every 18–22 min. Total activity, as measured by the number of x axis and z-axis beam breaks, was monitored every minute. For cytokine administration experiments, mice were placed in CLAMS two days after the last injection. For induced thermogenic capacity experiments, norepinephrine (1 mg/kg) was injected intraperitoneally into conscious mice, and VO_2 was measured every 4 min and normalized to each animal's preinjection baseline.

Adipocyte Progenitor Isolation and Culture

Subcutaneous WAT was digested, filtered, and washed as described above. Adipocyte progenitors were then isolated as per the manufacturer's MACS protocol (Miltenyi) using first negative selection of CD45 and CD31 followed by positive selection for SCA-1. Briefly, cell suspensions were incubated with Fc block followed by biotinylated antibodies against CD45 and CD31 followed by streptavidin-conjugated magnetic beads. Cells were then washed and passed over a lineage depletion column. The flow-through was collected, washed, and incubated with PE-conjugated anti-SCA-1 followed by anti-PE-conjugated magnetic beads. Cells were then washed and passed over a lineage selection column. Retained cells were eluted, counted, and cultured as previously described (Ohno et al., 2012). Briefly, APs were expanded in Advanced DMEM F12 with 10% fetal bovine serum (GIBCO) in 6 cm tissue culture plates at low confluency until ready for use. For differentiation experiments, cells were replated at 1–2 × 10^5 cells per well in 12-well plates and treated with IL-4 or vehicle as indicated. After treatment, cells were thoroughly washed, and the media was supplemented

with beige differentiation cocktail (2 μgml^{-1} dexamethasone, 0.5 mM IBMX, 0.5–1 μM rosiglitazone, 1 nM tri- iodothyronine, 125 μM indomethacin, and 5 μgml^{-1} insulin). Phase contrast and fluorescence images were acquired using an EVOS FL cell imaging system (Life Technologies).

Histology

All tissues were placed in 10% formalin for 4–24 hr after harvest followed by 20% sucrose in PBS at 4°C until processing. Tissues were processed, embedded in paraffin, sectioned at 5 μm, and stained with hematoxylin and eosin. Images were acquired on an Olympus BX41 with a Digital Sight DS-Fi1 camera (Nikon).

SUPPLEMENTAL REFERENCES

Ohno, H., Shinoda, K., Spiegelman, B.M., and Kajimura, S. (2012). PPARγ agonists induce a white-to-brown fat conversion through stabilization of PRDM16 protein. Cell Metab. *15*, 395–404.

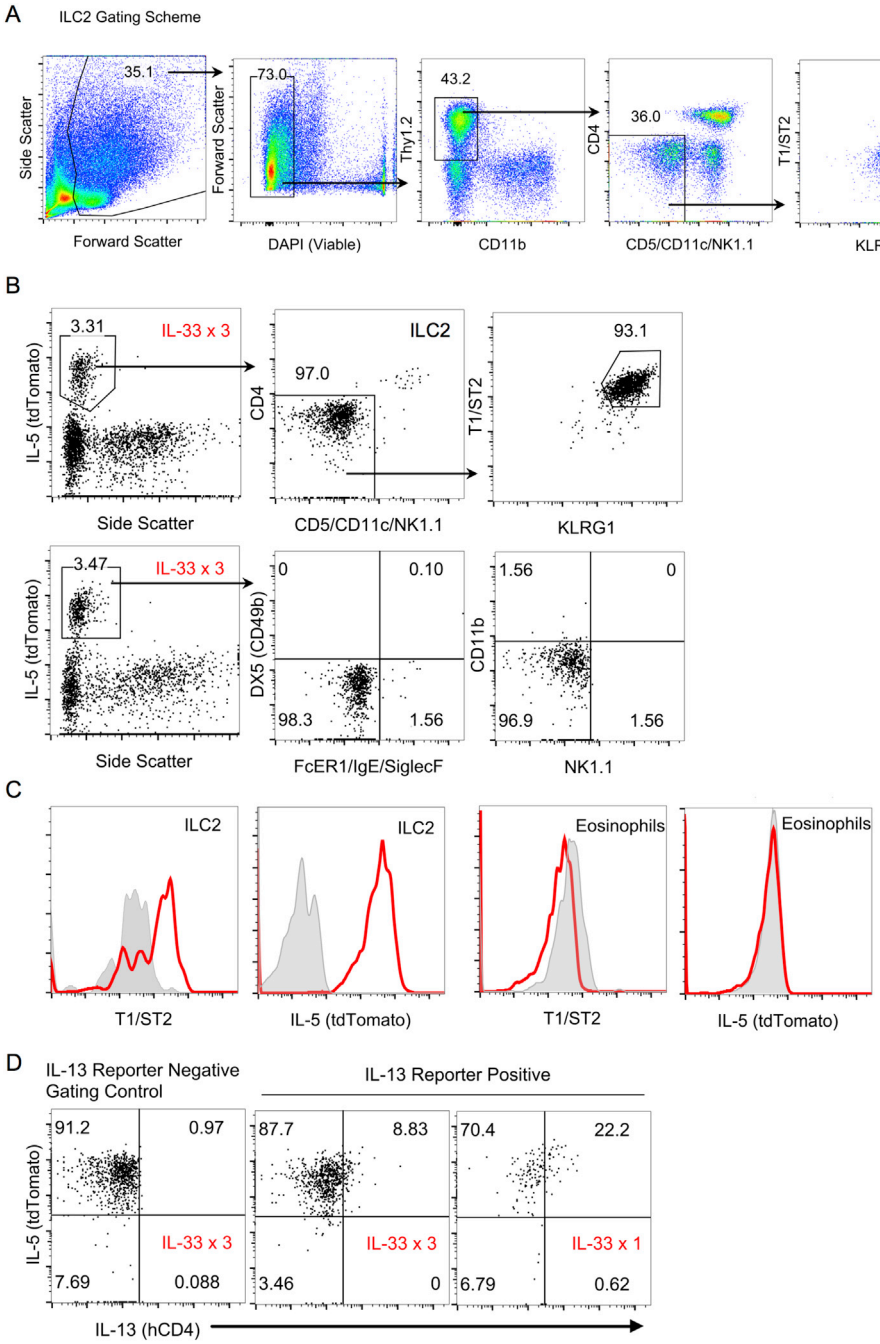

Figure S1. Flow Cytometric Analyses of ILC2s in the scWAT of Mice

(A) Gating strategy for the identification of ILC2s in heterozygous Red5 (*Il5*$^{Red5/+}$) mice administered IL-33. ILC2s were identified as Lin^{-} (CD11b^{-}CD4^{-}CD5^{-}Cd11c^{-}NK1.1^{-})Thy1.2^{+}T1/ST2^{+}KLRG1^{+} cells.

(B) Expression of IL-5 in scWAT cells. *Il5*$^{Red5/+}$ mice were administered IL-33 (3 doses administered every other) and IL-5 (tdTomato) cells were identified using the gating strategy described in S1A. Note that eosinophils, mast cells and basophils do not express IL-5 (tdTomato).

(C) Expression of T1/ST2 (IL-33Ra) and IL-5 in scWAT ILC2s and eosinophils of WT and *Il5*$^{Red5/+}$ mice treated with IL-33. For T1/ST2, gray histogram represents isotype staining and red histogram represents staining with T1/ST2 antibody. For IL-5 (tdTomato), gray histogram is representative of WT mice and red histogram is representative of *Il5*$^{Red5/+}$ mice.

(D) Quantification of IL-13 expression in scWAT ILC2s. R5 (*Il5*$^{Red5/+}$) and R5Smart13 (*Il5*$^{Red5/+}$*Il13*$^{Smart/+}$) mice were administered IL-33 (3 doses or a single dose), and expression of IL-13 was quantified in the scWAT ILC2s. In *Il5*$^{Red5/+}$*Il13*$^{Smart/+}$mice, nonsignaling human CD4 marks IL-13 producing cells.

See also Figure 2.

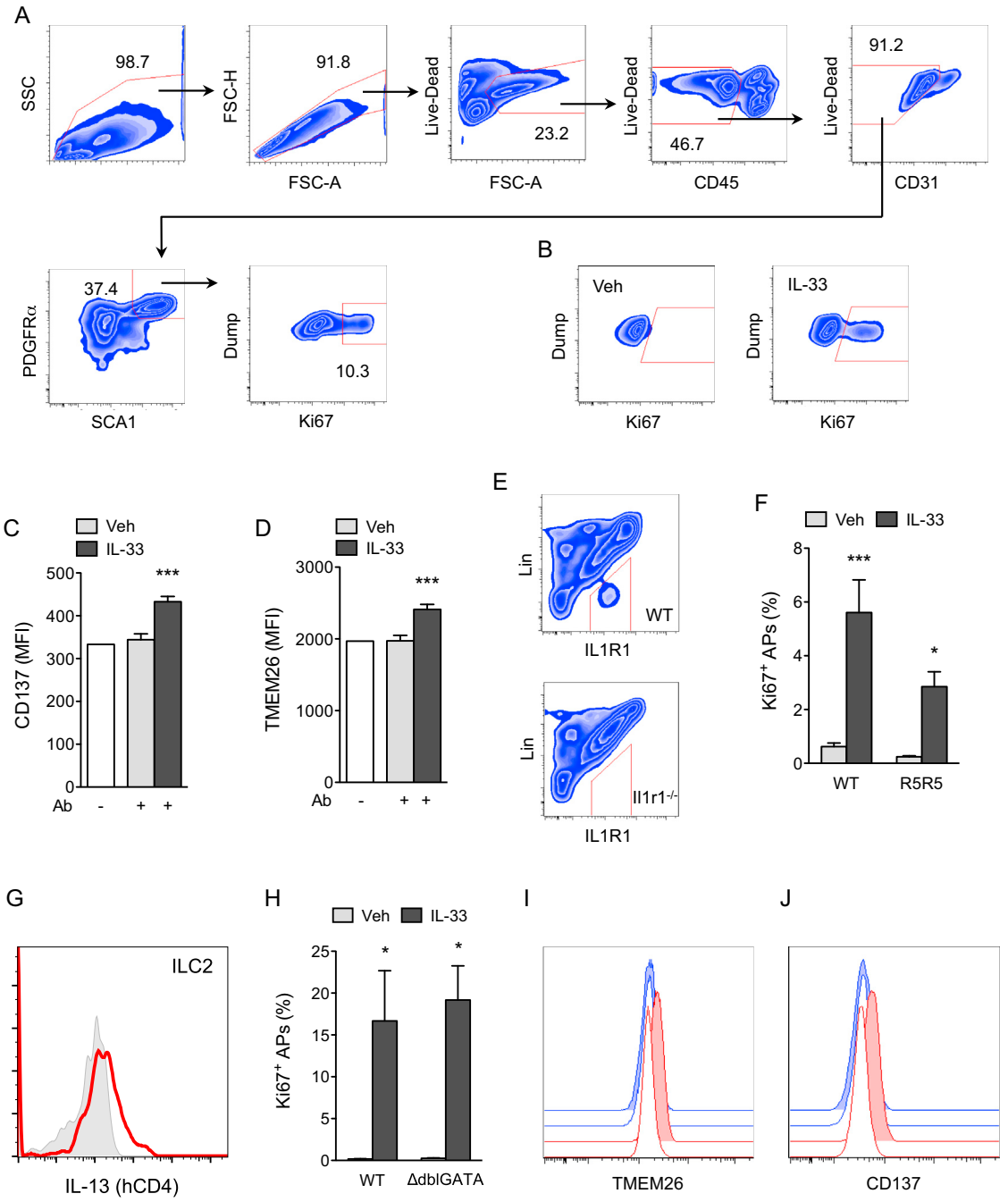

Figure S2. Flow Cytometric Analyses of APs in the scWAT of Mice

(A) Gating strategy for the identification of APs in scWAT of mice.

(B) Representative flow plots showing IL-33-induced proliferation of APs, as quantified by intracellular staining for Ki67.

(C) Quantification of beige adipocyte makers CD137 (C) and TMEM26 (D) on the scWAT APs of thermoneutral *Il5*$^{Red5/+}$ mice administered Veh or IL-33 for 8 days (n = 8–10 per treatment); antibody (Ab) refers to the presence or absence of primary antibody (n = 8–10 per treatment).

(E) Expression of IL1RL1 (IL-33R) on hematopoietic cells in wild-type (WT) and *Il1rl*$^{-/-}$ mice.

(F and H) Quantification of IL-33-induced AP proliferation in the scWAT of *Il5*$^{Red5/Red5}$ (F) and ΔdblGATA (H) mice (n = 4–8 per genotype and treatment).

(G) IL-33-induced expression of IL-13 in scWAT ILC2s of *Il5*$^{Red5/+}$ (gray histogram) and *Il5*$^{Red5/+}$*Il13*$^{Smart/+}$ (red histogram) mice.

(I and J) Representative histograms for TMEM26 (I) and CD137 (J) expression in the scWAT APs of *Rag2*$^{-/-}$ and *Rag2*$^{-/-}$*Il2rgc*$^{-/-}$ mice treated with Veh or IL-33. Red histograms- *Rag2*$^{-/-}$ scWAT APs, blue histograms- *Rag2*$^{-/-}$*Il2rgc*$^{-/-}$ scWAT APs; clear and shaded histograms represent Veh and IL-33 in each group. Data are represented as mean ± SEM. See also Figure 2.

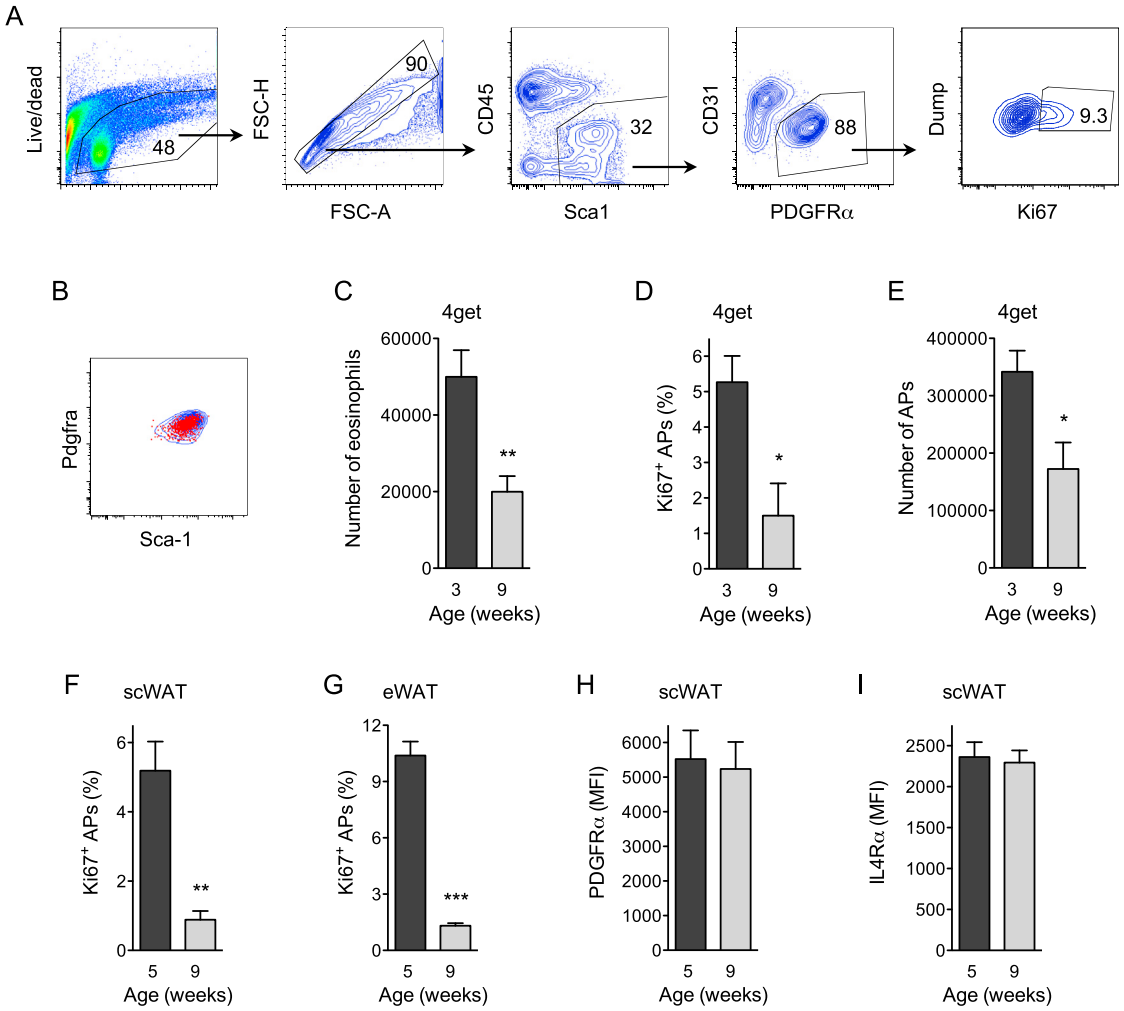

Figure S3. Analyses of APs in WAT of Mice at Various Ages

(A) Gating strategy for the identification of APs in the scWAT and eWAT of mice at various ages.

(B) Representative flow plot showing intracellular staining for Ki67 in PDGFRa^{+}SCA1^{+} APs in the scWAT. Ki67^{+} cells (Red) are overlaid on APs (Blue).

(C–E) Quantification of eosinophils (C), AP proliferation (D), and total AP number (E) in the scWAT of 3- and 9-week-old 4get mice (n = 5 per time point).

(F and G) Quantification of Ki67^{+} APs present in the scWAT (F) and eWAT (G) of 5- and 9-week-old BALB/cJ mice (n = 4–5 per time point).

(H and I) Expression of PDGFRα and IL4Rα in the scWAT APs of 5- and 9-week-old mice (n = 4–5 per time point).

Data are represented as mean ± SEM. See also Figure 3.

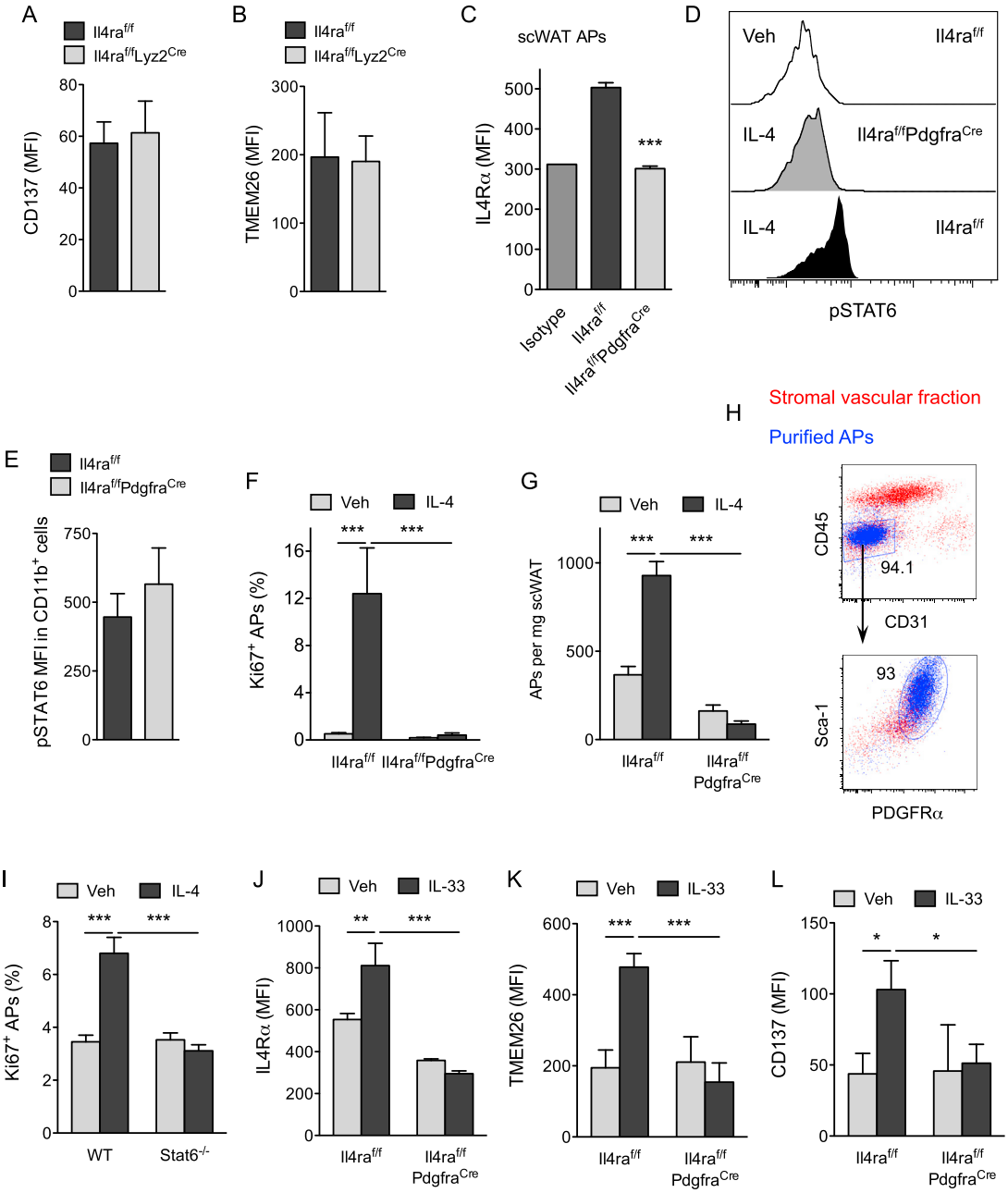

Figure S4. Requirement for IL-4Rα Signaling in PDGFRα$^+$ Cells for Proliferation of Adipogenic Precursors

(A and B) Expression of beige adipocyte precursor markers CD137 (A) and TMEM26 (B) on scWAT APs of *Il4ra*$^{f/f}$ and *Il4ra*$^{f/f}$*Lyz2*^{Cre} mice (n = 8–10 per genotype).

(C) Expression of IL4Rα on scWAT APs of *Il4ra*$^{f/f}$ and *Il4ra*$^{f/f}$*Pdgfra*^{Cre} mice (n = 3–4 per genotype).

(D and E) Analysis of IL-4-induced phosphorylation of STAT6 (pSTAT6) in scWAT APs (D) and CD11b$^+$ cells (E) of *Il4ra*$^{f/f}$ and *Il4ra*$^{f/f}$*Pdgfra*^{Cre} mice (n = 3–4 per genotype).

(F and G) Quantification of AP proliferation (F) and total number (G) in the scWAT of *Il4ra*$^{f/f}$ and *Il4ra*$^{f/f}$*Pdgfra*^{Cre} mice 48 hr after administration of vehicle or IL-4 (n = 4–6 per genotype and treatment).

(H) Flow cytometric analysis of APs purified from scWAT stromal vascular fraction of WT mice.

(I) APs purified from wild-type and *Stat6*$^{-/-}$ mice were stimulated with IL-4, and cellular proliferation was quantified by intracellular staining for Ki67 48 hr later (n = 4 per genotype and treatment).

(J–L) Expression of IL-4Rα (J), TMEM26 (K), and CD137 (L) in scWAT APs of *Il4ra*$^{f/f}$ and *Il4ra*$^{f/f}$*Pdgfra*^{Cre} mice treated with vehicle or IL-33 (n = 8–10 per genotype and treatment). Data are represented as mean ± SEM. See also Figure 4.

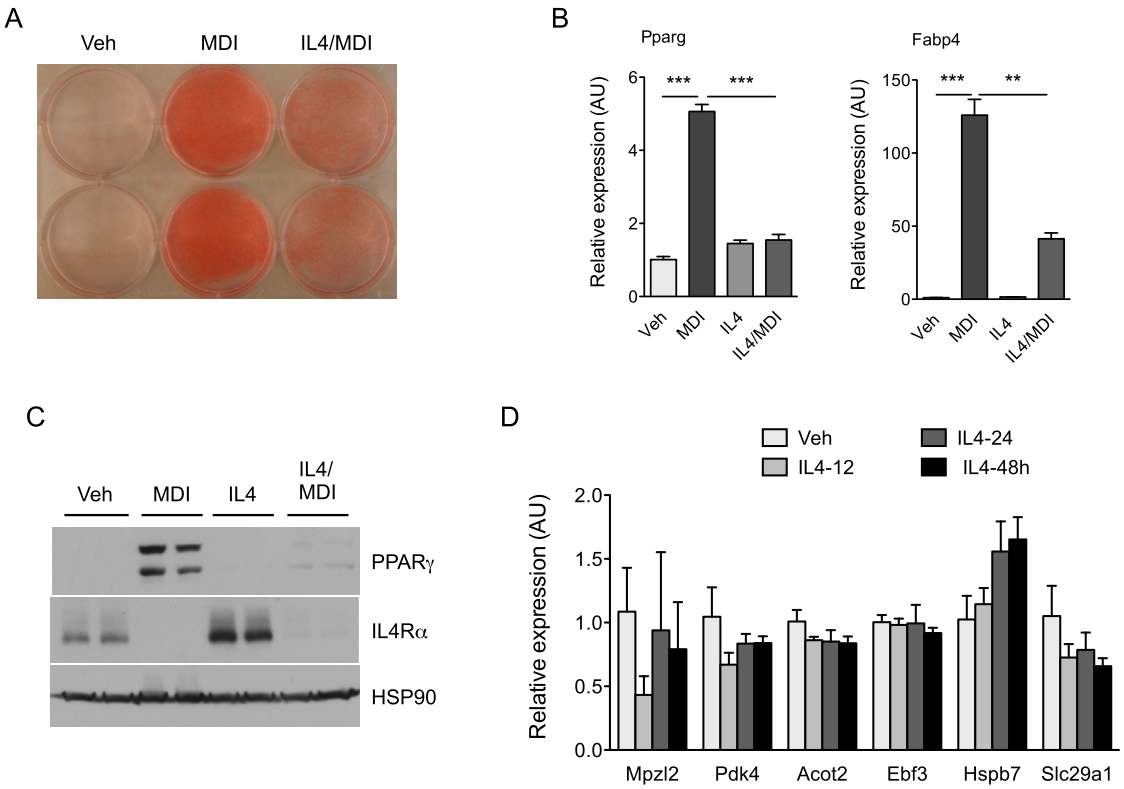

Figure S5. Effects of IL-4 on Differentiation of scWAT APs into White or Brown Adipocytes

(A–C) IL-4 inhibits the differentiation of scWAT APs into white adipocytes. Purified APs were treated with vehicle (Veh), adipogenic cocktail (MDI), or IL-4 for 48 hr followed by stimulation with MDI in the absence of IL-4. Oil red O staining (A), qRT-PCR analysis of adipogenic genes *Pparg* and *Fabp4* (n = 3 per treatment, data presented as mean ± SEM), and (C) immunoblot analysis of PPARγ and IL-4Rα.

(D) Expression of brown adipocyte markers in APs stimulated with IL-4 (n = 3 per treatment, data are represented as mean ± SD). See also Figure 5.

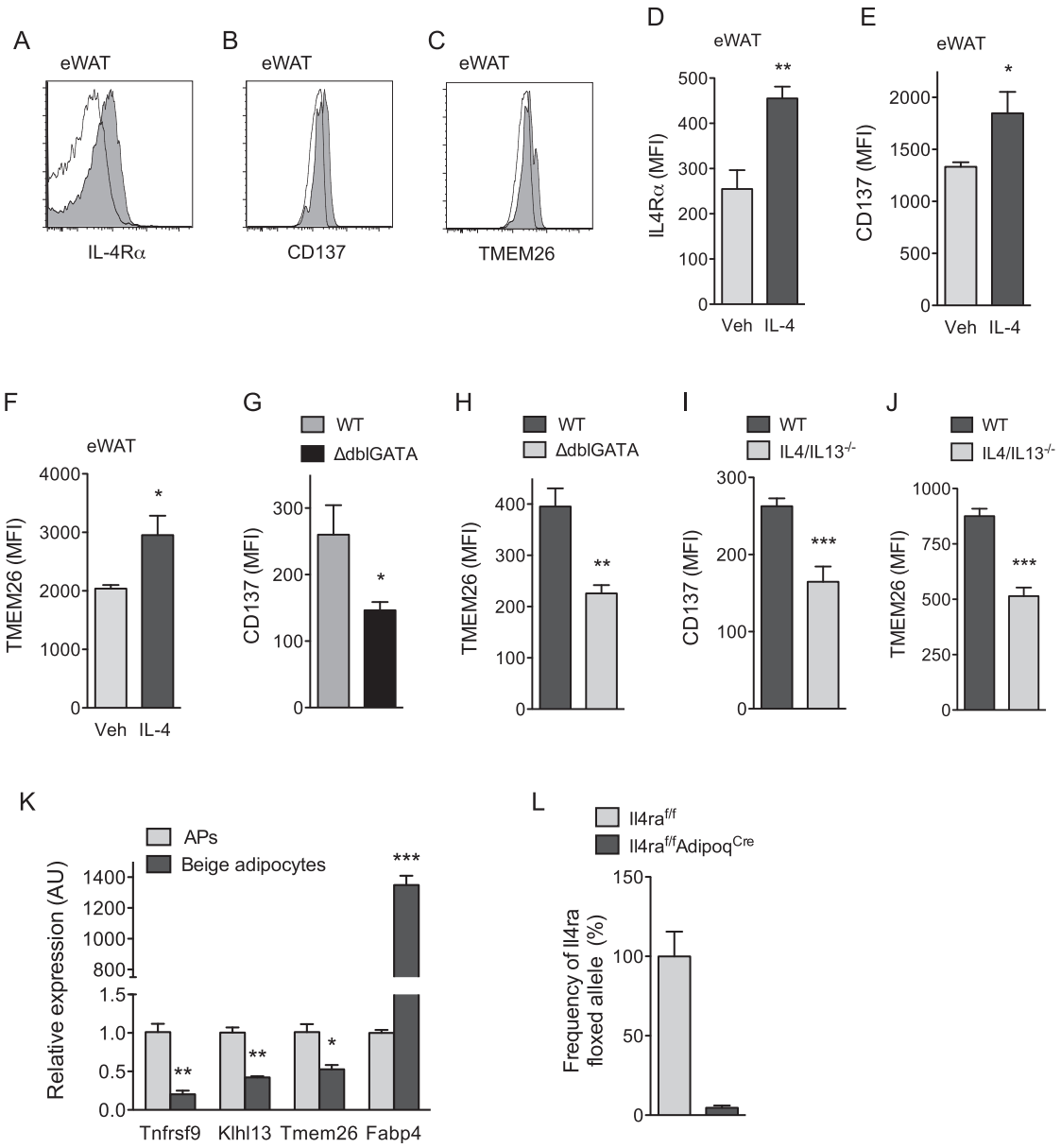

Figure S6. IL-4Rα Signaling Regulates Expression of Beige Adipocyte Precursor Markers in APs

(A–C) Flow cytometric analysis of IL-4Rα (A), CD137 (B), and TMEM26 (C) expression in eWAT APs of mice injected with vehicle or IL-4. Clear histogram: vehicle; gray histogram: IL-4.

(D–F) Quantification of IL-4Rα (D), CD137 (E), and TMEM26 (F) expression in eWAT APs 48 hr after administration of vehicle or IL-4 (n = 5 per treatment).

(G–J) Quantification of CD137 and TMEM26 expression in the scWAT APs of 5-week-old WT and ΔdblGATA mice (n = 6 per genotype, G, H) and WT and *Il4/13*$^{-/-}$ mice (n = 10 per genotype, I, J).

(K) Quantitative RT-PCR analysis of beige adipocyte markers in purified APs and in vitro differentiated beige adipocytes (n = 3 per group).

(L) Quantification of *Il4ra* floxed allele in purified mature adipocytes of *Il4ra*$^{f/f}$ and *Il4ra*$^{f/f}$*Adipoq*^{Cre} mice. Data are represented as mean ± SEM. See also Figures 5 and 7.